PTEP

Prog. Theor. Exp. Phys. **2015**, 013D02 (22 pages)
DOI: 10.1093/ptep/ptu172

Spin polarization versus color–flavor locking in high-density quark matter

Yasuhiko Tsue[1,2,*], João da Providência[2,†], Constança Providência[2,†], Masatoshi Yamamura[3,†], and Henrik Bohr[4,†]

[1]*Physics Division, Faculty of Science, Kochi University, Kochi 780-8520, Japan*
[2]*Center for Computational Physics, Departamento de Física, Universidade de Coimbra, 3004-516 Coimbra, Portugal*
[3]*Department of Pure and Applied Physics, Faculty of Engineering Science, Kansai University, Suita 564-8680, Japan*
[4]*Department of Physics, B.307, Danish Technical University, DK-2800 Lyngby, Denmark*
*E-mail: tsue@kochi-u.ac.jp

Received September 23, 2014; Revised November 11, 2014; Accepted November 26, 2014; Published January 22, 2015

It is shown that spin polarization with respect to each flavor in three-flavor quark matter occurs instead of color–flavor locking at high baryon density by using the Nambu–Jona-Lasinio model with four-point tensor-type interaction. Also, it is indicated that the order of phase transition between the color–flavor-locked phase and the spin-polarized phase is the first order by means of second-order perturbation theory.

Subject Index D30

1. Introduction

A recent point of interest in the physics governed by quantum chromodynamics (QCD) may be to understand the structure of the phase diagram on a plane with respect to, for example, temperature and baryon chemical potential or external magnetic field, isospin chemical potential, and so forth [1]. In particular, under extreme conditions such as high baryon density, it is interesting what phase is favorable and is realized. In the region with high baryon density and low temperature in quark matter, it is believed that there exists a two-flavor color superconducting (2SC) phase or the color–flavor-locked (CFL) phase [2]. In the preceding study, it was indicated that the spin-polarized phase may appear at high baryon density due to a pseudovector-type interaction between quarks [3–5]. However, in the limit of the quark mass being zero, it has been shown that the spin-polarized phase disappears [6].

In our preceding paper [7], it was shown that the quark spin-polarized (SP) phase in the two-flavor case is realized in the region of high baryon density by the use of the Nambu–Jona-Lasinio (NJL) model [8,9] devised by four-point tensor-type interaction with chiral symmetry [10]. Further, since the 2SC phase may exist in two-flavor QCD at high baryon density, it was also investigated whether the quark spin-polarized phase is realized or not against the 2SC phase. As a result, it was shown

[†]These authors contributed equally to this work.

Funded by SCOAP[3]

that the quark spin-polarized phase is actually realized in the same two-flavor NJL model adding to the quark-pair interaction [11].

In this paper, the possibility of quark spin polarization for each flavor is investigated in the three-flavor case by using the NJL model with four-point tensor-type interaction. In the three-flavor case, the CFL phase may be realized at high baryon density. Thus, the quark-pairing interaction is introduced and it is investigated which phase, namely the CFL phase or the SP phase, is favorable energetically and is realized at high baryon density. Also, if both phases exist, it is necessary to discuss the order of phase transition between the CFL and SP phases.

This paper is organized as follows: In the next section, the NJL-type model Hamiltonian is explained. In Sect. 3 with Appendix A, under the above-derived Hamiltonian, the CFL phase without the condensate of the quark spin polarization and/or the SP phase without the color superconducting gap are discussed. In Sect. 4, numerical results are given and the realized phase in certain density regions is considered. In Sect. 5, based on the CFL phase and dealing with tensor-type interaction as a perturbation term, the order of phase transition from the CFL phase to the SP phase is discussed. Some expressions needed in the calculation of second-order perturbation are given in Appendix B. he last section is devoted to a summary and concluding remarks.

2. Hamiltonian showing three-flavor color superconductivity and spin polarization based on the NJL model

Let us start with the following NJL-type Lagrangian density:

$$\mathcal{L} = \bar{\psi} i\gamma^\mu \partial_\mu \psi - \frac{G}{4}(\bar{\psi}\gamma^\mu\gamma^\nu\lambda_k^f\psi)(\bar{\psi}\gamma_\mu\gamma_\nu\lambda_k^f\psi) + \frac{G_c}{2}(\bar{\psi}i\gamma_5\lambda_a^c\lambda_k^f\psi^C)(\bar{\psi}^C i\gamma_5\lambda_a^c\lambda_k^f\psi), \quad (2.1)$$

where $\psi^C = C\bar{\psi}^T$ with $C = i\gamma^2\gamma^0$ being the charge conjugation operator. Also, λ_k^f and λ_a^c are the flavor and color $su(3)$ Gell-Mann matrices, respectively. Here, the NJL Lagrangian density contains other four-point interaction parts which are not explicitly shown such as $G_0(\bar{\psi}\psi)(\bar{\psi}\psi)$ and is invariant under chiral transformation. However, in this paper, some terms are omitted because we investigate only the condensates with respect to color–flavor locking and each quark-spin polarization in high density quark matter in the mean field approximation. For example, at high baryon density, the chiral condensate $\langle\bar{\psi}\psi\rangle$ is equal to zero. Further, in the three-flavor case, it is well known that the Kobayashi–Maskawa–'t Hooft (KMT) term [12,13] appears, which describes the $U_A(1)$ anomaly and is represented by the six-point interaction with determinant-type form in the NJL model. However, hereafter, since we adopt the mean field approximation, the KMT term only gives contributions such as $\langle\bar{\psi}_u\psi_u\rangle\langle\bar{\psi}_d\psi_d\rangle\langle\bar{\psi}_s\psi_s\rangle$, $\langle\bar{\psi}_d\psi_d\rangle\langle\bar{\psi}_s\psi_s\rangle(\bar{\psi}_u\psi_u)$, and so on, where ψ_f represents the quark field with flavor f and $\langle\cdots\rangle$ represents the condensate. Thus, at the high baryon density under investigation in this paper, there is no contribution of the KMT term because the chiral condensate $\langle\bar{\psi}_f\psi_f\rangle$ is zero. As for the quark masses, although the strange quark mass with 0.1 GeV is certainly nonzero compared with the up and down quark masses, we may safely ignore the strange quark mass at high baryon density with the quark chemical potential being 0.4–0.5 GeV under consideration in this paper. Thus, we ignore the quark mass term in (2.1).

Within the mean field approximation, the above Lagrangian density is expressed as

$$\mathcal{L}^{MF} = \bar{\psi} i\gamma^\mu \partial_\mu \psi + \mathcal{L}_T^{MF} + \mathcal{L}_c^{MF},$$

$$\mathcal{L}_T^{MF} = -\sum_{k=3,8} F_k(\bar{\psi}\Sigma_3\lambda_k^f\psi) - \frac{1}{2G}\sum_{k=3,8} F_k^2,$$

$$
\begin{aligned}
\Sigma_3 &= -i\gamma^1\gamma^2 = \begin{pmatrix} \sigma_3 & 0 \\ 0 & \sigma_3 \end{pmatrix}, \\
F_3 &= -G\langle\bar{\psi}\Sigma_3\lambda_3^f\psi\rangle, \quad F_8 = -G\langle\bar{\psi}\Sigma_3\lambda_8^f\psi\rangle, \\
\mathcal{F}_u &= F_3 + \frac{1}{\sqrt{3}}F_8, \quad \mathcal{F}_d = -F_3 + \frac{1}{\sqrt{3}}F_8, \quad \mathcal{F}_s = -\frac{2}{\sqrt{3}}F_8, \\
\mathcal{L}_c^{MF} &= -\frac{1}{2}\sum_{(a,k)=\{2,5,7\}}\left(\left(\Delta_{ak}^*(\bar{\psi}^C i\gamma_5\lambda_a^c\lambda_k^f\psi) + h.c.\right) + \frac{1}{2G_C}|\Delta_{ak}|^2\right), \\
\Delta_{ak} &= -G_c\langle\bar{\psi}^C i\gamma_5\lambda_a^c\lambda_k^f\psi\rangle,
\end{aligned} \tag{2.2}
$$

where $h.c.$ represents the Hermitian conjugate term of the preceding one. Here, we used the Dirac representation for the Dirac gamma matrices and σ_3 represents the third component of the 2×2 Pauli spin matrices. The symbol $\langle\cdots\rangle$ represents the expectation value with respect to a vacuum state. The expectation values F_3 and F_8 correspond to the order parameter of the spin alignment which may lead to quark spin polarization. The expectation value Δ_{ak} corresponds to the quark-pair condensate which means the existence of the color superconducting phase if $\Delta_{ak} \neq 0$.

The mean field Hamiltonian density with quark chemical potential μ is easily obtained as

$$
\begin{aligned}
\mathcal{H}_{MF} - \mu\mathcal{N} &= \mathcal{K}_0 + \mathcal{H}_T^{MF} + \mathcal{H}_c^{MF}, \\
\mathcal{K}_0 &= \bar{\psi}(-i\boldsymbol{\gamma}\cdot\nabla - \mu\gamma_0)\psi, \\
\mathcal{H}_T^{MF} &= -\mathcal{L}_T^{MF}, \quad \mathcal{H}_c^{MF} = -\mathcal{L}_c^{MF},
\end{aligned} \tag{2.3}
$$

with $\mathcal{N} = \psi^\dagger\psi$. In the Dirac representation for the Dirac gamma matrices, the Hamiltonian matrix of the spin polarization part in $H_{MF}^{SP} = \int d^3\boldsymbol{x}\ (\mathcal{K}_0 + \mathcal{H}_T^{MF})$ is written as

$$
\begin{aligned}
h_{MF}^{SP} &= \boldsymbol{p}\cdot\boldsymbol{\alpha} + \mathcal{F}_\tau\beta\Sigma_3 \\
&= \begin{pmatrix} \mathcal{F}_\tau & 0 & p_3 & p_1 - ip_2 \\ 0 & -\mathcal{F}_\tau & p_1 + ip_2 & p_3 \\ p_3 & p_1 - ip_2 & -\mathcal{F}_\tau & 0 \\ p_1 + ip_2 & -p_3 & 0 & \mathcal{F}_\tau \end{pmatrix},
\end{aligned} \tag{2.4}
$$

where $\alpha^i = \gamma^0\gamma^i$ and $\beta = \gamma^0$. Here, we define $\mathcal{F}_\tau$ as

$$
\mathcal{F}_\tau = \sum_{k=3,8} F_k\lambda_k^f = \left(F_3 + \frac{1}{\sqrt{3}}F_8\right)\delta_{\tau u} + \left(-F_3 + \frac{1}{\sqrt{3}}F_8\right)\delta_{\tau d} - \frac{2}{\sqrt{3}}F_8\delta_{\tau s}. \tag{2.5}
$$

For good helicity states, this Hamiltonian matrix is easily diagonalized in the case $\mathcal{F}_\tau = 0$. For simplicity, we rotate around the p_3 axis and we set $p_2 = 0$ without loss of generality. In this case, we derive $\kappa = U^{-1}h_{MF}^{SP}U$ as follows:

$$
U = \frac{1}{2\sqrt{p}}\begin{pmatrix} \sqrt{p+p_3} & \sqrt{p-p_3} & -\sqrt{p+p_3} & -\sqrt{p-p_3} \\ \frac{p_1}{|p_1|}\sqrt{p-p_3} & -\frac{p_1}{|p_1|}\sqrt{p+p_3} & -\frac{p_1}{|p_1|}\sqrt{p-p_3} & \frac{p_1}{|p_1|}\sqrt{p+p_3} \\ \sqrt{p+p_3} & -\sqrt{p-p_3} & \sqrt{p+p_3} & -\sqrt{p-p_3} \\ \frac{p_1}{|p_1|}\sqrt{p-p_3} & \frac{p_1}{|p_1|}\sqrt{p+p_3} & \frac{p_1}{|p_1|}\sqrt{p-p_3} & \frac{p_1}{|p_1|}\sqrt{p+p_3} \end{pmatrix},
$$

$$\kappa = U^{-1} h_{MF}^{SP} U$$
$$= \begin{pmatrix} p & 0 & 0 & 0 \\ 0 & p & 0 & 0 \\ 0 & 0 & -p & 0 \\ 0 & 0 & 0 & -p \end{pmatrix} + \frac{\mathcal{F}_\tau}{p} \begin{pmatrix} 0 & |p_1| & -p_3 & 0 \\ |p_1| & 0 & 0 & p_3 \\ -p_3 & 0 & 0 & |p_1| \\ 0 & p_3 & |p_1| & 0 \end{pmatrix}. \tag{2.6}$$

Finally, in the original basis rotated around the p_3 axis, $|p_1|$ is replaced by $\sqrt{p_1^2 + p_2^2}$. Thus, the many-body Hamiltonian can be expressed by means of the quark creation and annihilation operators as is seen later.

As for the Hamiltonian matrix of the color superconducting part, $H_c^{MF} = \int d^3\boldsymbol{x} \mathcal{H}_c^{MF}$, we can derive another expression by using the quark creation and annihilation operators with respect to good helicity states, similarly to Ref. [11]. As a result, in the basis of good helicity states, the relevant combination of the mean field Hamiltonian $H_{MF} = \int d^3\boldsymbol{x} \mathcal{H}_{MF}$ and the quark number $N = \int d^3\boldsymbol{x} \mathcal{N}$ is given by

$$H = H_0 - \mu\hat{N} + V_{\rm SP} + V_{\rm CFL} + V \cdot \frac{1}{2G}(F_3^2 + F_8^2) + V \cdot \frac{3\Delta^2}{2G_c},$$
$$H_0 - \mu\hat{N} = \sum_{\mathbf{p}\eta\tau\alpha} \left[(|\boldsymbol{p}| - \mu) c^\dagger_{\mathbf{p}\eta\tau\alpha} c_{\mathbf{p}\eta\tau\alpha} - (|\boldsymbol{p}| + \mu) \tilde{c}^\dagger_{\mathbf{p}\eta\tau\alpha} \tilde{c}^\dagger_{\mathbf{p}\eta\tau\alpha} \right],$$
$$V_{\rm SP} = \sum_{\mathbf{p}\eta\tau\alpha} \mathcal{F}_\tau \left[\frac{\sqrt{p_1^2 + p_2^2}}{|\boldsymbol{p}|} \left(c^\dagger_{\mathbf{p}\eta\tau\alpha} c_{\mathbf{p}-\eta\tau\alpha} + \tilde{c}^\dagger_{\mathbf{p}\eta\tau\alpha} \tilde{c}_{\mathbf{p}-\eta\tau\alpha} \right) - \eta \frac{p_3}{|\boldsymbol{p}|} \left(c^\dagger_{\mathbf{p}\eta\tau\alpha} \tilde{c}_{\mathbf{p}\eta\tau\alpha} + \tilde{c}^\dagger_{\mathbf{p}\eta\tau\alpha} c_{\mathbf{p}\eta\tau\alpha} \right) \right],$$
$$V_{\rm CFL} = \frac{\Delta}{2} \sum_{\mathbf{p}\eta} \sum_{\alpha\alpha'\alpha''} \sum_{\tau\tau'} \left(c^\dagger_{\mathbf{p}\eta\alpha\tau} c^\dagger_{-\mathbf{p}\eta\alpha'\tau'} + c_{-\mathbf{p}\eta\alpha'\tau'} c_{\mathbf{p}\eta\alpha\tau} + \tilde{c}^\dagger_{\mathbf{p}\eta\alpha\tau} \tilde{c}^\dagger_{-\mathbf{p}\eta\alpha'\tau'} + \tilde{c}_{-\mathbf{p}\eta\alpha'\tau'} \tilde{c}_{\mathbf{p}\eta\alpha\tau} \right)$$
$$\times \epsilon_{\alpha\alpha'\alpha''} \epsilon_{\tau\tau'\tau_{\alpha''}} \phi_p, \tag{2.7}$$

where V represents the volume in the box normalization. Here, $c^\dagger_{\boldsymbol{p}\eta\tau\alpha}$ and $\tilde{c}^\dagger_{\boldsymbol{p}\eta\tau\alpha}$ represent the quark and antiquark creation operators[1] with momentum $\boldsymbol{p}$, helicity $\eta = \pm$, flavor index τ, and color α. It should be noted that α $(= 1, 2, 3)$ and τ $(= u, d, s)$ represent color and flavor, respectively, and in particular we understand $\tau_1 = u$, $\tau_2 = d$, and $\tau_3 = s$. Hereafter, we will use $p \equiv (\boldsymbol{p}, \eta)$ and $\bar{p} \equiv (-\boldsymbol{p}, \eta)$ as abbreviated notations. Also, $\epsilon_{\tau\tau'\tau''}$ and $\epsilon_{\alpha\alpha'\alpha''}$ represent the complete antisymmetric tensor for the flavor and color indices. We define $p = \sqrt{p_1^2 + p_2^2 + p_3^2}$, that is, the magnitude of momentum. In (2.7), the color and flavor are locked due to $V_{\rm CFL}$. Namely, the combinations

[1] Here, it is necessary to introduce ϕ_p in (2.7) for the character of fermion operator $c_{\mathbf{p}\eta\tau\alpha}$ and $\tilde{c}_{\mathbf{p}\eta\tau\alpha}$. Namely, for example,

$$\sum_{\mathbf{p}\eta\{\alpha\}\{\tau\}} c^\dagger_{\mathbf{p}\eta\tau\alpha} c^\dagger_{-\mathbf{p}\eta\tau'\alpha'} \phi_p \epsilon_{\alpha\alpha'\alpha''} \epsilon_{\tau\tau'\tau_{\alpha''}} = \frac{1}{2} \sum_{\mathbf{p}\eta\{\alpha\}\{\tau\}} (c^\dagger_{\mathbf{p}\eta\tau\alpha} c^\dagger_{-\mathbf{p}\eta\tau'\alpha'} \phi_p + c^\dagger_{-\mathbf{p}\eta\tau\alpha} c^\dagger_{\mathbf{p}\eta\tau'\alpha'} \phi_{\bar{p}}) \epsilon_{\alpha\alpha'\alpha''} \epsilon_{\tau\tau'\tau_{\alpha''}}$$
$$= \frac{1}{2} \sum_{\mathbf{p}\eta\{\alpha\}\{\tau\}} (c^\dagger_{\mathbf{p}\eta\tau\alpha} c^\dagger_{-\mathbf{p}\eta\tau'\alpha'} \phi_p - c^\dagger_{\mathbf{p}\eta\tau'\alpha'} c^\dagger_{-\mathbf{p}\eta\tau\alpha} \phi_{\bar{p}}) \epsilon_{\alpha\alpha'\alpha''} \epsilon_{\tau\tau'\tau_{\alpha''}}$$
$$= \frac{1}{2} \sum_{\mathbf{p}\eta\{\alpha\}\{\tau\}} (c^\dagger_{\mathbf{p}\eta\tau\alpha} c^\dagger_{-\mathbf{p}\eta\tau'\alpha'} \phi_p - c^\dagger_{\mathbf{p}\eta\tau\alpha} c^\dagger_{-\mathbf{p}\eta\tau'\alpha'} \phi_{\bar{p}}) \epsilon_{\alpha\alpha'\alpha''} \epsilon_{\tau\tau'\tau_{\alpha''}}.$$

Thus, we find $\phi_p = -\phi_{\bar{p}}$ with $p = (\boldsymbol{p}, \eta)$ and $\bar{p} = (-\boldsymbol{p}, \eta)$.

$\langle c_{\bar{p}1u}c_{p2d}\rangle - \langle c_{\bar{p}1d}c_{p2u}\rangle$, $\langle c_{\bar{p}2d}c_{p3s}\rangle - \langle c_{\bar{p}2s}c_{p3d}\rangle$, and $\langle c_{\bar{p}3s}c_{p1u}\rangle - \langle c_{\bar{p}3u}c_{p1s}\rangle$ appear in the CFL condensate Δ, in which we define

$$\Delta_{\alpha''\tau_{\alpha''}} = G_c \sum_{\mathbf{p}\eta\alpha\alpha'} \sum_{\tau\tau'} \langle c_{-\mathbf{p}\eta\alpha'\tau'} c_{\mathbf{p}\eta\alpha\tau}\rangle \epsilon_{\alpha\alpha'\alpha''}\epsilon_{\tau\tau'\tau_{\alpha''}}\phi_p,$$
$$\Delta = \Delta_{1u} = \Delta_{2d} = \Delta_{3s}\ . \tag{2.8}$$

The symmetry $su(3)_{\rm CFL}$ remains because the symmetry-breaking pattern is $su(3)_c \otimes su(3)_f \to su(3)_{\rm CFL}$.

3. Color–flavor-locked phase without spin polarization and spin-polarized phase without color–flavor locking

3.1. *Color–flavor-locked phase without spin polarization*

Let us consider the case $F_k = 0$, which leads to the color superconductor without spin polarization [14,15]. The Hamiltonian is expressed as

$$H_{\rm eff} = H_0 - \mu\hat{N} + V_{\rm CFL} + V\cdot\frac{3\Delta^2}{2G_c},$$
$$H_0 - \mu\hat{N} = \sum_{\mathbf{p}\eta\tau\alpha}\left[(|\boldsymbol{p}| - \mu)c^\dagger_{\mathbf{p}\eta\tau\alpha}c_{\mathbf{p}\eta\tau\alpha} - (|\boldsymbol{p}| + \mu)\tilde{c}^\dagger_{\mathbf{p}\eta\tau\alpha}\tilde{c}^\dagger_{\mathbf{p}\eta\tau\alpha}\right],$$
$$V_{\rm CFL} = \frac{\Delta}{2}\sum_{\mathbf{p}\eta}\sum_{\alpha\alpha'\alpha''}\sum_{\tau\tau'}\left(c^\dagger_{\mathbf{p}\eta\alpha\tau}c^\dagger_{-\mathbf{p}\eta\alpha'\tau'} + c_{-\mathbf{p}\eta\alpha'\tau'}c_{\mathbf{p}\eta\alpha\tau} + \tilde{c}^\dagger_{\mathbf{p}\eta\alpha\tau}\tilde{c}^\dagger_{-\mathbf{p}\eta\alpha'\tau'} + \tilde{c}_{-\mathbf{p}\eta\alpha'\tau'}\tilde{c}_{\mathbf{p}\eta\alpha\tau}\right)$$
$$\times\,\epsilon_{\alpha\alpha'\alpha''}\epsilon_{\tau\tau'\tau_{\alpha''}}\phi_p. \tag{3.1}$$

Hereafter, we use an abbreviated notation $p = (\boldsymbol{p}, \eta)$ and $\bar{p} = (-\boldsymbol{p}, \eta)$. The commutation relations are calculated as

$$[H_{\rm eff}, c_{p1u}] = -(\epsilon_{pu} - \mu)c_{p1u} - \Delta(c^\dagger_{\bar{p}2d} + c^\dagger_{\bar{p}3s})\phi_p,$$
$$[H_{\rm eff}, c_{p2u}] = -(\epsilon_{pu} - \mu)c_{p2u} + \Delta c^\dagger_{\bar{p}1d}\phi_p,$$
$$[H_{\rm eff}, c_{p3u}] = -(\epsilon_{pu} - \mu)c_{p3u} + \Delta c^\dagger_{\bar{p}1s}\phi_p,$$
$$[H_{\rm eff}, c_{p1d}] = -(\epsilon_{pd} - \mu)c_{p1d} + \Delta c^\dagger_{\bar{p}2u}\phi_p,$$
$$[H_{\rm eff}, c_{p2d}] = -(\epsilon_{pd} - \mu)c_{p2d} - \Delta\left(c^\dagger_{\bar{p}3s} + c^\dagger_{\bar{p}1u}\right)\phi_p,$$
$$[H_{\rm eff}, c_{p3d}] = -(\epsilon_{pd} - \mu)c_{p3d} + \Delta c^\dagger_{\bar{p}2s}\phi_p,$$
$$[H_{\rm eff}, c_{p1s}] = -(\epsilon_{ps} - \mu)c_{p1s} + \Delta c^\dagger_{\bar{p}3u}\phi_p,$$
$$[H_{\rm eff}, c_{p2s}] = -(\epsilon_{ps} - \mu)c_{p2s} + \Delta c^\dagger_{\bar{p}3d}\phi_p,$$
$$[H_{\rm eff}, c_{p3s}] = -(\epsilon_{ps} - \mu)c_{p3s} - \Delta(c^\dagger_{\bar{p}1u} + c^\dagger_{\bar{p}2d})\phi_p, \tag{3.2}$$

where $\epsilon_{pu} = \epsilon_{pd} = \epsilon_{ps} = |\boldsymbol{p}|\ (= \epsilon_p)$. Thus, $(1u)$, $(2d)$, and $(3s)$ become combined with each other. Further, the sets $(2u, 1d)$, $(3u, 1s)$, and $(3d, 2s)$ are mixed each other. First, let us consider the case

$\varepsilon_{p\tau} > \mu$. Thus, for example, we are led to consider new operators such as the following one:

$$d^\dagger_{p2u} = X_p c^\dagger_{p2u} + Y_p c_{\bar{p}1d} \, . \tag{3.3}$$

Here, we demand that this operator should satisfy the following commutation relation in order to diagonalize the Hamiltonian $H_{\rm eff}$:

$$\begin{aligned}[H_{\rm eff}, d^\dagger_{p2u}] &= [(\epsilon_{pu} - \mu)X_p - \Delta Y_p \phi_p] c^\dagger_{p2u} + [-(\epsilon_{pd} - \mu)Y_p - \Delta X_p \phi_p] c_{\bar{p}1d} \\ &\equiv \omega \, d^\dagger_{p2u}. \end{aligned} \tag{3.4}$$

Then, X_p and Y_p are determined from the following equation:

$$\begin{pmatrix} \epsilon_p - \mu & -\Delta\phi_p \\ -\Delta\phi_p & -(\epsilon_p - \mu) \end{pmatrix} \begin{pmatrix} X_p \\ Y_p \end{pmatrix} = \omega \begin{pmatrix} X_p \\ Y_p \end{pmatrix}. \tag{3.5}$$

As a result, we can derive the following:

$$\begin{aligned} X_p &= \frac{1}{\sqrt{2}} \left[1 + \frac{\bar{\epsilon}_p}{\sqrt{\bar{\epsilon}_p^2 + \Delta^2}} \right]^{1/2}, \quad Y_p = -\frac{1}{\sqrt{2}} \left[1 - \frac{\bar{\epsilon}_p}{\sqrt{\bar{\epsilon}_p^2 + \Delta^2}} \right]^{1/2} \phi_p, \\ \omega_p &= \sqrt{\bar{\epsilon}_p^2 + \Delta^2}, \quad \bar{\epsilon}_p = \epsilon_p - \mu. \end{aligned} \tag{3.6}$$

Similarly, we can introduce new operators and the results are summarized as follows for $|\boldsymbol{p}| > \mu$:

$$\begin{aligned} d^\dagger_{p;1} &= x^{(1)}_p (c^\dagger_{p1u} + c^\dagger_{p2d} + c^\dagger_{p3s}) + y^{(1)}_p (c_{\bar{p}1u} + c_{\bar{p}2d} + c_{\bar{p}3s}), \\ x^{(1)}_p &= \frac{1}{\sqrt{6}} \left[1 + \frac{\bar{\epsilon}_p}{\sqrt{\bar{\epsilon}_p^2 + 4\Delta^2}} \right]^{1/2}, \quad y^{(1)}_p = \frac{1}{\sqrt{6}} \left[1 - \frac{\bar{\epsilon}_p}{\sqrt{\bar{\epsilon}_p^2 + 4\Delta^2}} \right]^{1/2} \cdot \phi_p, \\ \omega_1 &= \sqrt{\bar{\epsilon}_p^2 + 4\Delta^2}, \\ d^\dagger_{p;2} &= x^{(2)}_p (c^\dagger_{p1u} - c^\dagger_{p2d}) + y^{(2)}_p (c_{\bar{p}1u} - c_{\bar{p}2d}), \\ x^{(2)}_p &= \frac{1}{2} \left[1 + \frac{\bar{\epsilon}_p}{\sqrt{\bar{\epsilon}_p^2 + \Delta^2}} \right]^{1/2}, \quad y^{(2)}_p = -\frac{1}{2} \left[1 - \frac{\bar{\epsilon}_p}{\sqrt{\bar{\epsilon}_p^2 + \Delta^2}} \right]^{1/2} \cdot \phi_p, \\ \omega_2 &= \sqrt{\bar{\epsilon}_p^2 + \Delta^2}, \\ d^\dagger_{p;3} &= x^{(3)}_p (c^\dagger_{p1u} + c^\dagger_{p2d} - 2c^\dagger_{p3s}) + y^{(3)}_p (c_{\bar{p}1u} + c_{\bar{p}2d} - 2c_{\bar{p}3s}), \\ x^{(3)}_p &= \frac{1}{2\sqrt{3}} \left[1 + \frac{\bar{\epsilon}_p}{\sqrt{\bar{\epsilon}_p^2 + \Delta^2}} \right]^{1/2}, \quad y^{(3)}_p = -\frac{1}{2\sqrt{3}} \left[1 - \frac{\bar{\epsilon}_p}{\sqrt{\bar{\epsilon}_p^2 + \Delta^2}} \right]^{1/2} \cdot \phi_p, \end{aligned}$$

$$
\begin{aligned}
\omega_3 &= \sqrt{\bar{\epsilon}_p^2 + \Delta^2}, \\
d_{p;4} &= d_{p2u}^\dagger = X_p c_{p2u}^\dagger + Y_p c_{\bar{p}1d}, \quad d_{p;5} = d_{p1d}^\dagger = X_p c_{p1d}^\dagger + Y_p c_{\bar{p}2u}, \\
d_{p;6} &= d_{p3u}^\dagger = X_p c_{p3u}^\dagger + Y_p c_{\bar{p}1s}, \quad d_{p;7} = d_{p1s}^\dagger = X_p c_{p1s}^\dagger + Y_p c_{\bar{p}3u}, \\
d_{p;8} &= d_{p3d}^\dagger = X_p c_{p3d}^\dagger + Y_p c_{\bar{p}2s}, \quad d_{p;9} = d_{p2s}^\dagger = X_p c_{p2s}^\dagger + Y_p c_{\bar{p}3d}, \\
X_p &= \frac{1}{\sqrt{2}} \left[1 + \frac{\bar{\epsilon}_p}{\sqrt{\bar{\epsilon}_p^2 + \Delta^2}} \right]^{1/2}, \quad Y_p = -\frac{1}{\sqrt{2}} \left[1 - \frac{\bar{\epsilon}_p}{\sqrt{\bar{\epsilon}_p^2 + \Delta^2}} \right]^{1/2} \cdot \phi_p, \\
\omega &= \sqrt{\bar{\epsilon}_p^2 + \Delta^2},
\end{aligned} \tag{3.7}
$$

where $\bar{\epsilon}_p = |\boldsymbol{p}| - \mu$, $y_{\bar{p}}^{(i)} = -y_p^{(i)}$, and $Y_{\bar{p}} = -Y_p$. Inversely, we can derive the following:

$$
\begin{aligned}
c_{p1u}^\dagger &= x_p^{(1)} d_{p;1}^\dagger + x_p^{(2)} d_{p;2}^\dagger + x_p^{(3)} d_{p;3}^\dagger - (y_p^{(1)} d_{\bar{p};1} + y_p^{(2)} d_{\bar{p};2} + y_p^{(3)} d_{\bar{p};3}), \\
c_{p2d}^\dagger &= x_p^{(1)} d_{p;1}^\dagger - x_p^{(2)} d_{p;2}^\dagger + x_p^{(3)} d_{p;3}^\dagger - (y_p^{(1)} d_{\bar{p};1} - y_p^{(2)} d_{\bar{p};2} + y_p^{(3)} d_{\bar{p};3}), \\
c_{p3s}^\dagger &= x_p^{(1)} d_{p;1}^\dagger - 2x_p^{(3)} d_{p;3}^\dagger - (y_p^{(1)} d_{\bar{p};1} - 2y_p^{(3)} d_{\bar{p};3}), \\
c_{p2u}^\dagger &= X_p d_{p2u}^\dagger - Y_p d_{\bar{p}1d}, \quad c_{p1d}^\dagger = X_p d_{p1d}^\dagger - Y_p d_{\bar{p}2u}, \quad c_{p3u}^\dagger = X_p d_{p3u}^\dagger - Y_p d_{\bar{p}1s}, \\
c_{p1s}^\dagger &= X_p d_{p1s}^\dagger - Y_p d_{\bar{p}3u}, \quad c_{p3d}^\dagger = X_p d_{p3d}^\dagger - Y_p d_{\bar{p}2s}, \quad c_{p2s}^\dagger = X_p d_{p2s}^\dagger - Y_p d_{\bar{p}3d}.
\end{aligned} \tag{3.8}
$$

As for $\epsilon_p < \mu$ with $\epsilon_p = |\boldsymbol{p}|$, we can introduce the new operators in a similar way to the case of $\epsilon_p > \mu$. The new operators, $\bar{d}_{\bar{p};i}$, satisfy diagonalized commutation relations such as

$$
[H_{\text{eff}}, \bar{d}_{\bar{p};i}] = -\omega_i \bar{d}_{\bar{p};i}, \tag{3.9}
$$

where $\omega_4 = \omega_5 = \cdots = \omega_9 = \omega$. Then, the new operators can be derived as

$$
\begin{aligned}
\bar{d}_{\bar{p};1} &= \bar{x}_p^{(1)} (c_{p1u}^\dagger + c_{p2d}^\dagger + c_{p3s}^\dagger) + \bar{y}_p^{(1)} (c_{\bar{p}1u} + c_{\bar{p}2d} + c_{\bar{p}3s}), \\
\bar{x}_p^{(1)} &= \frac{1}{\sqrt{6}} \left[1 - \frac{\bar{\epsilon}_p}{\sqrt{\bar{\epsilon}_p^2 + 4\Delta^2}} \right]^{1/2}, \quad \bar{y}_p^{(1)} = -\frac{1}{\sqrt{6}} \left[1 + \frac{\bar{\epsilon}_p}{\sqrt{\bar{\epsilon}_p^2 + 4\Delta^2}} \right]^{1/2} \cdot \phi_p, \\
\omega_1 &= \sqrt{\bar{\epsilon}_p^2 + 4\Delta^2}, \\
\bar{d}_{\bar{p};2} &= \bar{x}_p^{(2)} (c_{p1u}^\dagger - c_{p2d}^\dagger) + \bar{y}_p^{(2)} (c_{\bar{p}1u} - c_{\bar{p}2d}), \\
\bar{x}_p^{(2)} &= \frac{1}{2} \left[1 - \frac{\bar{\epsilon}_p}{\sqrt{\bar{\epsilon}_p^2 + \Delta^2}} \right]^{1/2}, \quad \bar{y}_p^{(2)} = \frac{1}{2} \left[1 + \frac{\bar{\epsilon}_p}{\sqrt{\bar{\epsilon}_p^2 + \Delta^2}} \right]^{1/2} \cdot \phi_p, \\
\omega_2 &= \sqrt{\bar{\epsilon}_p^2 + \Delta^2}, \\
\bar{d}_{\bar{p};3} &= \bar{x}_p^{(3)} (c_{p1u}^\dagger + c_{p2d}^\dagger - 2c_{p3s}^\dagger) + \bar{y}_p^{(3)} (c_{\bar{p}1u} + c_{\bar{p}2d} - 2c_{\bar{p}3s}),
\end{aligned}
$$

$$
\begin{aligned}
&\bar{x}_p^{(3)} = \frac{1}{2\sqrt{3}}\left[1 - \frac{\bar{\epsilon}_p}{\sqrt{\bar{\epsilon}_p^2 + \Delta^2}}\right]^{1/2}, \quad \bar{y}_p^{(3)} = \frac{1}{2\sqrt{3}}\left[1 + \frac{\bar{\epsilon}_p}{\sqrt{\bar{\epsilon}_p^2 + \Delta^2}}\right]^{1/2} \cdot \phi_p, \\
&\omega_3 = \sqrt{\bar{\epsilon}_p^2 + \Delta^2}, \\
&\bar{d}_{\bar{p};4} = \bar{d}_{\bar{p}2u} = \bar{X}_p c_{p2u}^\dagger + \bar{Y}_p c_{\bar{p}1d}, \quad \bar{d}_{\bar{p};5} = \bar{d}_{\bar{p}1d} = \bar{X}_p c_{p1d}^\dagger + \bar{Y}_p c_{\bar{p}2u}, \\
&\bar{d}_{\bar{p};6} = \bar{d}_{\bar{p}3u} = \bar{X}_p c_{p3u}^\dagger + \bar{Y}_p c_{\bar{p}1s}, \quad \bar{d}_{\bar{p};7} = \bar{d}_{\bar{p}1s} = \bar{X}_p c_{p1s}^\dagger + \bar{Y}_p c_{\bar{p}3u}, \\
&\bar{d}_{\bar{p};8} = \bar{d}_{\bar{p}3d} = \bar{X}_p c_{p3d}^\dagger + \bar{Y}_p c_{\bar{p}2s}, \quad \bar{d}_{\bar{p};9} = \bar{d}_{\bar{p}2s} = \bar{X}_p c_{p2s}^\dagger + \bar{Y}_p c_{\bar{p}3d}, \\
&\bar{X}_p = \frac{1}{\sqrt{2}}\left[1 - \frac{\bar{\epsilon}_p}{\sqrt{\bar{\epsilon}_p^2 + \Delta^2}}\right]^{1/2}, \quad \bar{Y}_p = \frac{1}{\sqrt{2}}\left[1 + \frac{\bar{\epsilon}_p}{\sqrt{\bar{\epsilon}_p^2 + \Delta^2}}\right]^{1/2} \cdot \phi_p, \\
&\omega = \sqrt{\bar{\epsilon}_p^2 + \Delta^2}.
\end{aligned} \tag{3.10}
$$

The following inverse relations are obtained:

$$
\begin{aligned}
&c_{p1u}^\dagger = \bar{x}_p^{(1)}\bar{d}_{\bar{p};1} + \bar{x}_p^{(2)}\bar{d}_{\bar{p};2} + \bar{x}_p^{(3)}\bar{d}_{\bar{p};3} - (\bar{y}_p^{(1)}\bar{d}_{p;1}^\dagger + \bar{y}_p^{(2)}\bar{d}_{p;2}^\dagger + \bar{y}_p^{(3)}\bar{d}_{p;3}^\dagger), \\
&c_{p2d}^\dagger = \bar{x}_p^{(1)}\bar{d}_{\bar{p};1} - \bar{x}_p^{(2)}\bar{d}_{\bar{p};2} + \bar{x}_p^{(3)}\bar{d}_{\bar{p};3} - (\bar{y}_p^{(1)}\bar{d}_{p;1}^\dagger - \bar{y}_p^{(2)}\bar{d}_{p;2}^\dagger + \bar{y}_p^{(3)}\bar{d}_{p;3}^\dagger), \\
&c_{p3s}^\dagger = \bar{x}_p^{(1)}\bar{d}_{\bar{p};1} - 2\bar{x}_p^{(3)}\bar{d}_{\bar{p};3} - (\bar{y}_p^{(1)}\bar{d}_{p;1}^\dagger - 2\bar{y}_p^{(3)}\bar{d}_{p;3}^\dagger), \\
&c_{p2u}^\dagger = \bar{X}_p\bar{d}_{\bar{p}2u} - \bar{Y}_p\bar{d}_{p1d}^\dagger, \quad c_{p1d}^\dagger = \bar{X}_p\bar{d}_{\bar{p}1d} - \bar{Y}_p\bar{d}_{p2u}^\dagger, \quad c_{p3u}^\dagger = \bar{X}_p\bar{d}_{\bar{p}3u} - \bar{Y}_p\bar{d}_{p1s}^\dagger, \\
&c_{p1s}^\dagger = \bar{X}_p\bar{d}_{\bar{p}1s} - \bar{Y}_p\bar{d}_{p3u}^\dagger, \quad c_{p3d}^\dagger = \bar{X}_p\bar{d}_{\bar{p}3d} - \bar{Y}_p\bar{d}_{p2s}^\dagger, \quad c_{p2s}^\dagger = \bar{X}_p\bar{d}_{\bar{p}2s} - \bar{Y}_p\bar{d}_{p3d}^\dagger.
\end{aligned} \tag{3.11}
$$

By using the above operators, we rewrite $H_{\rm eff}$ as is shown in (A1) in Appendix A. Noting X_p etc. in (3.7) and (3.10), we finally obtain the following diagonalized many-body Hamiltonian without spin polarization:

$$
\begin{aligned}
H_{\rm eff} = &\frac{1}{2}\sum_{p\ (\epsilon_p>\mu)}\left[9\bar{\epsilon}_p - \sqrt{\bar{\epsilon}_p^2 + 4\Delta^2} - 8\sqrt{\bar{\epsilon}_p^2 + \Delta^2}\right] \\
&+ \sum_{p\ (\epsilon_p>\mu)}\left[\sqrt{\bar{\epsilon}_p^2 + 4\Delta^2}\,d_{p;1}^\dagger d_{p;1} + \sum_{a=2}^{9}\sqrt{\bar{\epsilon}_p^2 + \Delta^2}\,d_{p;a}^\dagger d_{p;a}\right] \\
&+ \frac{1}{2}\sum_{p\ (\epsilon_p<\mu)}\left[9\bar{\epsilon}_p - \sqrt{\bar{\epsilon}_p^2 + 4\Delta^2} - 8\sqrt{\bar{\epsilon}_p^2 + \Delta^2}\right] \\
&+ \sum_{p\ (\epsilon_p<\mu)}\left[\sqrt{\bar{\epsilon}_p^2 + 4\Delta^2}\,\bar{d}_{p;1}^\dagger \bar{d}_{p;1} + \sum_{a=2}^{9}\sqrt{\bar{\epsilon}_p^2 + \Delta^2}\,\bar{d}_{p;a}^\dagger \bar{d}_{p;a}\right] + V\cdot\frac{3\Delta^2}{2G_c}.
\end{aligned} \tag{3.12}
$$

Next, let us derive and solve the gap equation for the CFL phase with $F_3 = F_8 = 0$ to obtain Δ. The vacuum state is written as $|\Phi\rangle$, which is a vacuum with respect to the quasi-particle operators $d_{p;a}$ and $\bar{d}_{p;a}$:

$$
d_{p;a}|\Phi\rangle = \bar{d}_{p;a}|\Phi\rangle = 0\,. \tag{3.13}
$$

Thus, the thermodynamic potential Φ_0 can be expressed as

$$\begin{aligned}\Phi_0 &= \frac{1}{V}\cdot\langle\Phi|H_{\rm eff}|\Phi\rangle \\ &= \frac{1}{2V}\sum_{p\ (\epsilon_p>\mu)}\left[9\bar{\epsilon}_p-\sqrt{\bar{\epsilon}_p^2+4\Delta^2}-8\sqrt{\bar{\epsilon}_p^2+\Delta^2}\right] \\ &\quad+\frac{1}{2V}\sum_{p\ (\epsilon_p<\mu)}\left[9\bar{\epsilon}_p-\sqrt{\bar{\epsilon}_p^2+4\Delta^2}-8\sqrt{\bar{\epsilon}_p^2+\Delta^2}\right]+\frac{3\Delta^2}{2G_c}.\end{aligned} \tag{3.14}$$

The gap equation, $\partial\Phi_0/\partial\Delta=0$, can be expressed as

$$\Delta\left(\frac{3}{G_c}-\int^{\Lambda}\frac{d^3\boldsymbol{p}}{(2\pi)^3}\left(\frac{4}{\sqrt{\bar{\epsilon}_p^2+4\Delta^2}}+\frac{8}{\sqrt{\bar{\epsilon}_p^2+\Delta^2}}\right)\right)=0, \tag{3.15}$$

where Λ represents a three-momentum cutoff. Here, the helicity $\eta=\pm1$ is considered which gives a factor 2. Namely, the above gap equation with $\Delta\neq0$ is written as

$$1=\frac{2G_c}{3\pi^2}\int_0^{\Lambda}dp\ p^2\left(\frac{1}{\sqrt{(p-\mu)^2+4\Delta^2}}+\frac{2}{\sqrt{(p-\mu)^2+\Delta^2}}\right), \tag{3.16}$$

where $p=|\boldsymbol{p}|$. Solving (3.16) with respect to Δ and substituting its solution into (3.14), the thermodynamic potential (3.14) is obtained:

$$\Phi_0=\frac{1}{2\pi^2}\int_0^{\Lambda}dp\ p^2\left(9(p-\mu)-\sqrt{(p-\mu)^2+4\Delta^2}-8\sqrt{(p-\mu)^2+\Delta^2}\right)+\frac{3\Delta^2}{2G_c}. \tag{3.17}$$

The right-hand sides of Eqs. (3.16) and (3.17) can be analytically expressed using the following formulae:

$$\begin{aligned}\int_0^{\Lambda}dp\frac{p^2}{\sqrt{(p-\mu)^2+c\Delta^2}} &= \left[\frac{p+3\mu}{2}\sqrt{p^2-2\mu p+\mu^2+c\Delta^2}\right]_0^{\Lambda} \\ &\quad+\left[\left(\mu^2-\frac{c\Delta^2}{2}\right)\ln\left|2p-2\mu+2\sqrt{p^2-2\mu p+\mu^2+c\Delta^2}\right|\right]_0^{\Lambda}, \\ \int_0^{\Lambda}dp\ p^2\sqrt{(p-\mu)^2+c\Delta^2} &= \left[\frac{3p+5\mu}{12}(p^2-2\mu p+\mu^2+c\Delta^2)^{3/2}\right]_0^{\Lambda} \\ &\quad+\left[\frac{4\mu^2-c\Delta^2}{8}\left((p-\mu)\sqrt{p^2-2\mu p+\mu^2+c\Delta^2}\right.\right. \\ &\quad\left.\left.+\ c\Delta^2\ln\left|2p-2\mu+2\sqrt{p^2-2\mu p+\mu^2+c\Delta^2}\right|\right)\right]_0^{\Lambda}.\end{aligned} \tag{3.18}$$

Of course, if $\Delta=0$, the thermodynamic potential is given by

$$\Phi_0(\Delta=0)=-\frac{3\mu^4}{8\pi^2}. \tag{3.19}$$

3.2. *Spin-polarized phase without color superconducting gap* Δ

In this subsection, we derive the thermodynamic potential with $\Delta = 0$. In this case, it is only necessary to diagonalize the Hamiltonian matrix (2.6), namely,

$$\kappa = \begin{pmatrix} p & 0 & 0 & 0 \\ 0 & p & 0 & 0 \\ 0 & 0 & -p & 0 \\ 0 & 0 & 0 & -p \end{pmatrix} + \frac{\mathcal{F}_\tau}{p} \begin{pmatrix} 0 & \sqrt{p_1^2+p_2^2} & -p_3 & 0 \\ \sqrt{p_1^2+p_2^2} & 0 & 0 & p_3 \\ -p_3 & 0 & 0 & \sqrt{p_1^2+p_2^2} \\ 0 & p_3 & \sqrt{p_1^2+p_2^2} & 0 \end{pmatrix}$$
$$= \begin{pmatrix} q & e_\tau & -g_\tau & 0 \\ e_\tau & q & 0 & g_\tau \\ -g_\tau & 0 & -q & e_\tau \\ 0 & g_\tau & e_\tau & -q \end{pmatrix}, \tag{3.20}$$

where $q = p$, $e_\tau = \mathcal{F}_\tau\sqrt{p_1^2+p_2^2}/p$, and $g_\tau = \mathcal{F}_\tau p_3/p$. The eigenvalues of κ are easily obtained as

$$\pm\epsilon_{\boldsymbol{p}\tau}^{(\eta)} = \pm\sqrt{g_\tau^2 + (e_\tau + \eta q)^2} = \pm\sqrt{p_3^2 + \left(\mathcal{F}_\tau + \eta\sqrt{p_1^2+p_2^2}\right)^2}, \tag{3.21}$$

where $\mathcal{F}_\tau$ are defined in (2.5) or (2.2). Since the Hamiltonian is diagonalized, the thermodynamic potential with $\Delta = 0$, which is written as Φ_F, can be easily obtained as

$$\Phi_F = 3\frac{1}{V}\sum_{\boldsymbol{p}}\sum_{\eta=\pm}\sum_{\tau=u,d,s}(\epsilon_{\boldsymbol{p}\tau}^{(\eta)} - \mu)\theta(\mu - \epsilon_{\boldsymbol{p}\tau}^{(\eta)}) + \frac{1}{2G}(F_3^2 + F_8^2), \tag{3.22}$$

where the factor 3 represents the degree of freedom of color. Here, the sum with respect to the momentum should be replaced by the integration of momentum: $(1/V)\cdot\sum_{\boldsymbol{p}} \to \int d^3\boldsymbol{p}$. Hereafter, we assume $|\mathcal{F}_\tau| < \mu$ because we are interested in the phase transition from the CFL phase to the SP phase. In the case $0 \le \mathcal{F}_\tau < \mu$, the ranges of integration are obtained as:

for $\eta = -1$,

$$0 \le p_\perp = \sqrt{p_1^2+p_2^2} \le \mathcal{F}_\tau + \mu, \quad -\sqrt{\mu^2 - (\mathcal{F}_\tau - p_\perp)^2} \le p_3 \le \sqrt{\mu^2 - (\mathcal{F}_\tau - p_\perp)^2},$$

for $\eta = 1$,

$$0 \le p_\perp = \sqrt{p_1^2+p_2^2} \le \mu - \mathcal{F}_\tau, \quad -\sqrt{\mu^2 - (\mathcal{F}_\tau + p_\perp)^2} \le p_3 \le \sqrt{\mu^2 - (\mathcal{F}_\tau + p_\perp)^2}. \tag{3.23}$$

In the case $-\mu < \mathcal{F}_\tau \le 0$, the ranges of integration are obtained as:

for $\eta = -1$,

$$0 \le p_\perp = \sqrt{p_1^2+p_2^2} \le \mu - |\mathcal{F}_\tau|, \quad -\sqrt{\mu^2 - (|\mathcal{F}_\tau| + p_\perp)^2} \le p_3 \le \sqrt{\mu^2 - (|\mathcal{F}_\tau| + p_\perp)^2},$$

for $\eta = 1$,

$$0 \le p_\perp = \sqrt{p_1^2+p_2^2} \le |\mathcal{F}_\tau| + \mu, \quad -\sqrt{\mu^2 - (|\mathcal{F}_\tau| - p_\perp)^2} \le p_3 \le \sqrt{\mu^2 - (|\mathcal{F}_\tau| - p_\perp)^2}. \tag{3.24}$$

Regardless of the sign of $\mathcal{F}_\tau$, positive or negative, $\mathcal{F}_\tau$ is regarded as the absolute value of $\mathcal{F}_\tau$ since we consider both $\eta = 1$ and $\eta = -1$. Thus, from (3.22) and (3.23) or (3.24), the thermodynamic

potential can be expressed similarly to Eqn. (29) in Ref. [11]:

$$\begin{aligned}\Phi_F &= \frac{1}{2G}(F_3^2+F_8^2)\\ &\quad+\frac{3}{2\pi^2}\sum_\tau\Bigg[\int_0^{\mu-|\mathcal{F}_\tau|}dp_\perp\, p_\perp\int_0^{\sqrt{\mu^2-(|\mathcal{F}_\tau|+p_\perp)^2}}dp_3\left(\sqrt{p_3^2+(|\mathcal{F}_\tau|+p_\perp)^2}-\mu\right)\\ &\qquad+\int_0^{\mu+|\mathcal{F}_\tau|}dp_\perp\, p_\perp\int_0^{\sqrt{\mu^2-(|\mathcal{F}_\tau|-p_\perp)^2}}dp_3\left(\sqrt{p_3^2+(|\mathcal{F}_\tau|-p_\perp)^2}-\mu\right)\Bigg]\\ &= \frac{1}{2G}(F_3^2+F_8^2)\\ &\quad-\frac{1}{2\pi^2}\sum_\tau\left[\frac{\sqrt{\mu^2-\mathcal{F}_\tau^2}}{4}(3\mathcal{F}_\tau^2\mu+2\mu^3)+\mathcal{F}_\tau\mu^3\arctan\left(\frac{\mathcal{F}_\tau}{\sqrt{\mu^2-\mathcal{F}_\tau^2}}\right)\right.\\ &\qquad\left.-\frac{\mathcal{F}_\tau^4}{8}\ln\left(\frac{(\mu+\sqrt{\mu^2-\mathcal{F}_\tau^2})^2}{\mathcal{F}_\tau^2}\right)\right],\end{aligned}\tag{3.25}$$

where $\mathcal{F}_u = F_3 + F_8/\sqrt{3}$, $\mathcal{F}_d = -F_3 + F_8/\sqrt{3}$, and $\mathcal{F}_s = -2F_8/\sqrt{3}$. The simultaneous gap equations with respect to F_3 and F_8 are obtained through $\partial\Phi_F/\partial F_3 = 0$ and $\partial\Phi_F/\partial F_8 = 0$ as

$$\begin{aligned}\frac{\partial\Phi_F}{\partial F_k} &= \frac{F_k}{G}-\frac{1}{2\pi^2}\sum_{\tau=u,d,s}\left(2\mathcal{F}_\tau\mu\sqrt{\mu^2-\mathcal{F}_\tau^2}+\mu^3\arctan\left(\frac{\mathcal{F}_\tau}{\sqrt{\mu^2-\mathcal{F}_\tau^2}}\right)\right.\\ &\qquad\left.-\frac{\mathcal{F}_\tau^3}{2}\ln\left(\frac{(\mu+\sqrt{\mu^2-\mathcal{F}_\tau^2})^2}{\mathcal{F}_\tau^2}\right)\right)\cdot\frac{\partial\mathcal{F}_\tau}{\partial F_k}\\ &= 0,\end{aligned}\tag{3.26}$$

where $k = 3$ or 8 and $\partial\mathcal{F}_u/\partial F_3 = 1$, $\partial\mathcal{F}_d/\partial F_3 = -1$, $\partial\mathcal{F}_s/\partial F_3 = 0$, $\partial\mathcal{F}_u/\partial F_8 = 1/\sqrt{3}$, $\partial\mathcal{F}_d/\partial F_8 = 1/\sqrt{3}$, and $\partial\mathcal{F}_s/\partial F_8 = -2/\sqrt{3}$. Inserting the solutions of the simultaneous gap equations above into the thermodynamic potential Φ_F, we can estimate Φ_F, which should be compared with Φ_0 in (3.17). By comparing (3.25) with (3.17), the realized phase is determined.

4. Numerical results

Let us calculate the thermodynamic potential Φ_0 with $F_k = 0$ in (3.14) and Φ_F with $\Delta = 0$ in (3.22) or (3.25) numerically. If $\Phi_F < \Phi_0$, the SP phase is realized. However, in rather smaller μ, the CFL phase should be realized. The numerical results are summarized in Table 1. We adopt the parameters as $\Lambda = 0.631\,\mathrm{GeV}$, $G_c = 6.6\,\mathrm{GeV}^{-2}$, and $G = 20\,\mathrm{GeV}^{-2}$. As is seen in Table 1, in the region of $\mu \leq 0.45\,\mathrm{GeV}$, $\Phi_0 < \Phi_F$ is satisfied and the CFL phase is realized. At $\mu = 0.4558\,\mathrm{GeV}$ $(= \mu_c)$, $\Phi_0 \approx \Phi_F$ is satisfied. Thus, the phase transition may occur. In the region of $\mu \geq 0.46\,\mathrm{GeV}$, $\Phi_0 > \Phi_F$ is satisfied and the realized phase is the SP phase.

As for the solutions of the simultaneous gap equations in (3.26), it seems that the relation $F_3 \approx \sqrt{3}F_8$ may be satisfied. If $F_3 = \sqrt{3}F_8$, the relation $\mathcal{F}_d = \mathcal{F}_s(= -2F_3/3)$ is derived. In this case, $\mathcal{F}_u = 4F_3/3(= -2\mathcal{F}_d)$. As for another case, for example, $F_3 = 0$ and $F_8 \neq 0$, then $\mathcal{F}_u = \mathcal{F}_d$ and $\mathcal{F}_s = -2\mathcal{F}_u$ are satisfied. So, another local minimum may be obtained at $(F_3 = 0,\ F_8)$.

Table 1. The thermodynamic potentials Φ_0 with $F_k = 0$ and $\Delta \neq 0$, and Φ_F with $\Delta = 0$ and $F_k \neq 0$ are numerically given at each chemical potential μ.

μ/GeV	Δ/GeV	Φ_0/GeV^4	F_3/GeV	F_8/GeV	Φ_F/GeV^4
0.40	0.042640	−0.0020336	0	0	−0.0019454
0.41	0.045135	−0.0022509	0.048509	0.028007	−0.0021481
0.42	0.047509	−0.0024845	0.098544	0.056895	−0.0023753
0.43	0.049748	−0.0027352	0.136983	0.079087	−0.0026327
0.44	0.051841	−0.0030034	0.170908	0.098674	−0.0029245
0.45	0.053774	−0.0032897	0.202345	0.116824	−0.0032542
0.4558	0.054817	−0.0034643	0.219828	0.126918	−0.0034643
0.46	0.055536	−0.0035947	0.232234	0.134080	−0.0036256
0.47	0.057116	−0.0039189	0.261119	0.150757	−0.0040423
0.48	0.058502	−0.0042627	0.289365	0.167065	−0.0045084
0.49	0.059681	−0.0046267	0.317255	0.183167	−0.0050277
0.50	0.060640	−0.0050113	0.345041	0.199210	−0.0056046

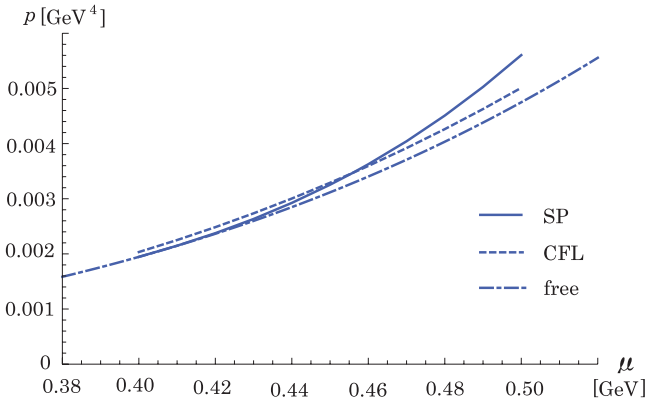

Fig. 1. The pressures for ($\Delta \neq 0$, $F_3 = F_8 = 0$; CFL), ($\Delta = 0$, $F_3 \neq 0$, $F_8 \neq 0$); SP), and free quark gas (free) are depicted as functions of the quark chemical potential μ.

Of course, the pressure p_A can be expressed by the thermodynamic potential Φ_A through the thermodynamical relation:

$$p_A = -\Phi_A. \tag{4.1}$$

In Fig. 1, the pressures of the CFL phase and the SP phase are depicted as a function of the chemical potential μ in comparison to that of the free quark matter. In $\mu < \mu_c$ ($\mu > \mu_c$), the pressure of the CFL phase is larger (smaller) than that of SP phase. Thus, the realized phase is CFL (SP) phase.

Also, the quark number density ρ_q can be derived from the thermodynamic potential by the thermodynamical relation

$$\rho_q = -\frac{\partial \Phi}{\partial \mu}. \tag{4.2}$$

The baryon number density ρ_B can be expressed as $\rho_B = \rho_q/3$. In Table 2, we summarize the baryon density and baryon density divided by the normal nuclear density $\rho_0 = 0.17\ \mathrm{fm}^{-3}$.

Finally, let us estimate the spin polarization. Here, we consider the helicity instead of spin. The quark number density for the flavor τ and helicity η can be derived as

$$n_\tau^{(\eta)} = 3 \int \frac{d^3\boldsymbol{p}}{(2\pi)^3} \theta(\mu - \epsilon_{\boldsymbol{p}\tau}^{(\eta)}), \tag{4.3}$$

Table 2. The pressures p_0 with $F_k = 0$ and p_F with $\Delta = 0$ are numerically calculated. The corresponding baryon number density ρ_B together with ρ_B/ρ_0, where ρ_0 represents the normal nuclear density, are given at each chemical potential μ.

μ/GeV	$\rho_B(F=0)/\mathrm{fm}^{-3}$	$\rho_B(F=0)/\rho_0$	p_0/GeV^4	$\rho_B(\Delta=0)/\mathrm{fm}^{-3}$	$\rho_B(\Delta=0)/\rho_0$	p_F/GeV^4
0.40	2.73681	5.36630	0.0020336	—	—	—
0.41	2.94752	5.77946	0.0022509	2.79121	5.47297	0.0021481
0.42	3.16606	6.20796	0.0024845	3.16045	6.19697	0.0023753
0.43	3.39217	6.65131	0.0027352	3.58384	7.02714	0.0016327
0.44	3.62561	7.10904	0.0030034	4.05631	7.95354	0.0029245
0.45	3.86614	7.58067	0.0032897	4.57688	8.97428	0.0032542
0.4558	4.00881	7.8604	0.0034643	4.90099	9.60978	0.0034643
0.46	4.11353	8.06574	0.0035947	5.14599	10.0902	0.0036256
0.47	4.36753	8.56379	0.0039189	5.76482	11.3036	0.0040423
0.48	4.62793	9.07438	0.0042627	6.43516	12.618	0.0045084
0.49	4.8945	9.59706	0.0046267	7.1594	14.038	0.0050277
0.50	5.16702	10.1314	0.0050113	7.94077	15.5701	0.0056046

where the factor 3 means color degree of freedom. First, in the case of $\mathcal{F}_\tau$ being positive and $0 < \mathcal{F}_\tau < \mu$, the particle number density with helicity $\pm$, $n^{(\pm)}_{\tau>}$, can be calculated as

$$\begin{aligned} n^{(+)}_{\tau>} &= \frac{3}{2\pi^2}\int_0^{\mu-\mathcal{F}_\tau} dp_\perp p_\perp \int_0^{\sqrt{\mu^2-(\mathcal{F}_\tau+p_\perp)^2}} dp_3 \\ &= \frac{1}{4\pi^2}\left[\sqrt{\mu^2-\mathcal{F}_\tau^2}(\mathcal{F}_\tau^2+2\mu^2) + 3\mathcal{F}_\tau\mu^2 \arctan\frac{\mathcal{F}_\tau}{\sqrt{\mu^2-\mathcal{F}_\tau^2}} - \frac{3\mathcal{F}_\tau\mu^2\pi}{2}\right], \\ n^{(-)}_{\tau>} &= \frac{3}{2\pi^2}\int_0^{\mu+\mathcal{F}_\tau} dp_\perp p_\perp \int_0^{\sqrt{\mu^2-(\mathcal{F}_\tau-p_\perp)^2}} dp_3 \\ &= \frac{1}{4\pi^2}\left[\sqrt{\mu^2-\mathcal{F}_\tau^2}(\mathcal{F}_\tau^2+2\mu^2) + 3\mathcal{F}_\tau\mu^2 \arctan\frac{\mathcal{F}_\tau}{\sqrt{\mu^2-\mathcal{F}_\tau^2}} + \frac{3\mathcal{F}_\tau\mu^2\pi}{2}\right]. \end{aligned} \tag{4.4}$$

On the other hand, in the case $-\mu < \mathcal{F}_\tau < 0$, the particle number density $n^{(\eta)}_{\tau<}$ is calculated as

$$\begin{aligned} n^{(+)}_{\tau<} &= \frac{3}{2\pi^2}\int_0^{\mu+|\mathcal{F}_\tau|} dp_\perp p_\perp \int_0^{\sqrt{\mu^2-(|\mathcal{F}_\tau|-p_\perp)^2}} dp_3 \\ &= \frac{1}{4\pi^2}\left[\sqrt{\mu^2-|\mathcal{F}_\tau|^2}(|\mathcal{F}_\tau|^2+2\mu^2) + 3|\mathcal{F}_\tau|\mu^2 \arctan\frac{|\mathcal{F}_\tau|}{\sqrt{\mu^2-|\mathcal{F}_\tau|^2}} + \frac{3|\mathcal{F}_\tau|\mu^2\pi}{2}\right], \\ n^{(-)}_{\tau<} &= \frac{3}{2\pi^2}\int_0^{\mu-|\mathcal{F}_\tau|} dp_\perp p_\perp \int_0^{\sqrt{\mu^2-(|\mathcal{F}_\tau|+p_\perp)^2}} dp_3 \\ &= \frac{1}{4\pi^2}\left[\sqrt{\mu^2-|\mathcal{F}_\tau|^2}(|\mathcal{F}_\tau|^2+2\mu^2) + 3|\mathcal{F}_\tau|\mu^2 \arctan\frac{|\mathcal{F}_\tau|}{\sqrt{\mu^2-|\mathcal{F}_\tau|^2}} - \frac{3|\mathcal{F}_\tau|\mu^2\pi}{2}\right]. \end{aligned} \tag{4.5}$$

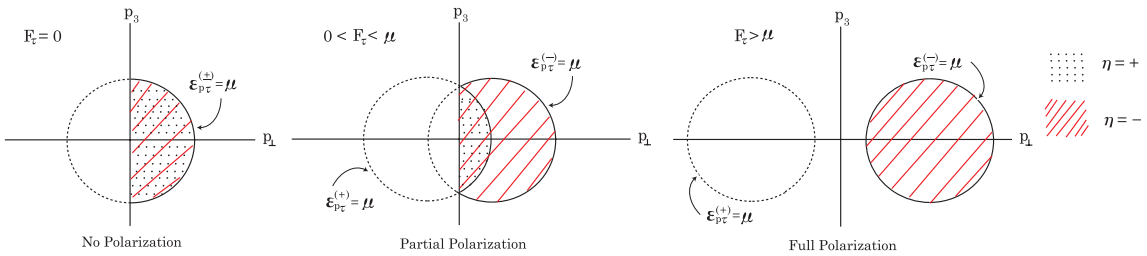

Fig. 2. The Fermi surface is depicted for $\mathcal{F}_\tau > 0$. In this case, the negative helicity dominates.

For the case $\mathcal{F}_\tau > \mu$, there is no contribution to the spin polarization from $\epsilon^{(+)}_{\boldsymbol{p}\tau}$ due to the integration range. Thus, we obtain only $n^{(-)}_{\tau>}$:

$$n^{(-)}_{\tau>} = 3\int \frac{d^3\boldsymbol{p}}{(2\pi)^3}\theta\left(\mu - \epsilon^{(-)}_{\boldsymbol{p}\tau}\right) = \frac{3\mu^2}{4\pi}\mathcal{F}_\tau. \tag{4.6}$$

It should be noted here that the Fermi surface has the form of a torus in the case $\mathcal{F}_\tau > \mu$, namely, $(\sqrt{p_1^2 + p_2^2} - \mathcal{F}_\tau)^2 + p_3^2 = \mu^2$, whose volume is obtained as $2\pi\mathcal{F}_\tau \times \pi\mu^2$ where $\mathcal{F}_\tau$ and μ correspond to the major and minor radii of the torus. For the case $\mathcal{F}_\tau < -\mu$, similar to Eqn. (4.6), we obtain the following:

$$n^{(+)}_{\tau<} = \frac{3\mu^2}{4\pi}|\mathcal{F}_\tau|. \tag{4.7}$$

Next, let us consider the case $|\mathcal{F}_\tau| < \mu$. The spin polarization per unit volume is obtained by the difference between the quark number with the positive helicity and that with the negative helicity, as shown in Fig. 2. Further, we assume that $\mathcal{F}_u > 0$, $\mathcal{F}_d < 0$, and $\mathcal{F}_s < 0$. The spin polarization of each flavor, $\mathcal{S}_\tau$, can be expressed as

$$\mathcal{S}_u/(\hbar/2) = n^{(+)}_{u>} - n^{(-)}_{u>} = -\frac{3}{4\pi}\mathcal{F}_u\mu^2\,. \tag{4.8}$$

Similarly,

$$\mathcal{S}_d/(\hbar/2) = n^{(+)}_{d<} - n^{(-)}_{d<} = \frac{3}{4\pi}|\mathcal{F}_d|\mu^2, \quad \mathcal{S}_s/(\hbar/2) = n^{(+)}_{s<} - n^{(-)}_{s<} = \frac{3}{4\pi}|\mathcal{F}_s|\mu^2. \tag{4.9}$$

Of course, the total spin polarization $\mathcal{S}$ is written as

$$\mathcal{S} = \mathcal{S}_u + \mathcal{S}_d + \mathcal{S}_s. \tag{4.10}$$

Figure 3 shows the numerical results. For d- and s-quarks, the spin polarization has almost the same magnitude. On the other hand, for the u-quark, the spin polarization is opposite to d- and s-quarks. The total spin polarization is nearly equal to zero. The reason is as follows: From the numerical calculation, the condensate F_3 and F_8 satisfy the relation $F_3 \approx \sqrt{3}F_8$, which makes the thermodynamic potential a minimum. Under this relation, $\mathcal{F}_u = -2\mathcal{F}_d$ and $\mathcal{F}_d = \mathcal{F}_s$ are satisfied. Thus, from (4.8)–(4.10), $\mathcal{S} = 0$ is derived.

5. The order of phase transition and the second-order perturbation with respect to $V_{\rm SP}$

In order to investigate the order of phase transition from CFL phase to SP phase, we treat the interaction term $V_{\rm SP}$ in the perturbation theory on the vacuum of the CFL phase. We neglect the contribution

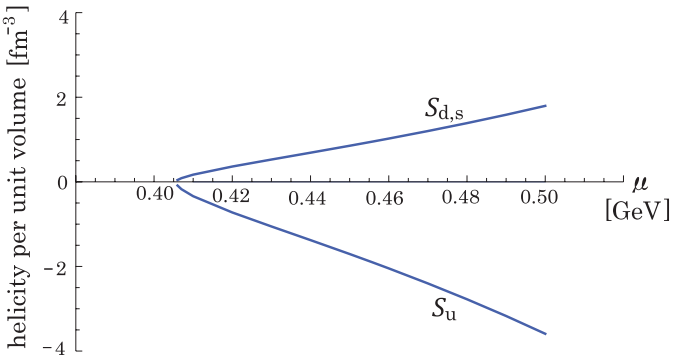

Fig. 3. The spin polarization of each flavor is depicted as a function of the quark chemical potential μ.

of the negative-energy particle represented by $(\tilde{c}_{p\tau\alpha}, \tilde{c}^{\dagger}_{p\tau\alpha})$. Thus, in V_{SP} in (2.7), it is enough to pick up only the following term:

$$H_1 = \sum_{\boldsymbol{p}\eta\tau\alpha} \mathcal{F}_\tau \frac{\sqrt{p_1^2+p_2^2}}{|\boldsymbol{p}|} c^{\dagger}_{\boldsymbol{p}\eta\tau\alpha} c_{\boldsymbol{p}-\eta\tau\alpha} = \sum_{\boldsymbol{p}\eta\tau\alpha} e_\tau c^{\dagger}_{\boldsymbol{p}\eta\tau\alpha} c_{\boldsymbol{p}-\eta\tau\alpha},$$
$$e_\tau \equiv \mathcal{F}_\tau \frac{\sqrt{p_1^2+p_2^2}}{|\boldsymbol{p}|}. \tag{5.1}$$

The correction of the first-order perturbation with respect to H_1, namely $\langle\Phi|H_1|\Phi\rangle$, vanishes because the helicity η is different from each other like $\langle\Phi|d_{\boldsymbol{p}\eta;a} d^{\dagger}_{\boldsymbol{p}-\eta;a}|\Phi\rangle = 0$, which comes from $\langle\Phi|c^{\dagger}_{\boldsymbol{p}\eta\tau\alpha} c_{\boldsymbol{p}-\eta\tau\alpha}|\Phi\rangle$. Thus, we need to calculate the second-order perturbation with respect to H_1. The correction of energy can be expressed as

$$E_{\mathrm{corr}} = \sum_i \frac{\langle\Phi|H_1|i\rangle\langle i|H_1|\Phi\rangle}{E_0 - E_i}, \tag{5.2}$$

where $|i\rangle$, E_0, and E_i represent the excited state, the vacuum energy, and the excited energies, respectively. The term H_1 includes $c^{\dagger}_{\boldsymbol{p}\eta\alpha\tau} c_{\boldsymbol{p}-\eta\alpha\tau}$. For example, in the case $\epsilon_p > \mu$ with $\tau = u$, the necessary term can be expressed in terms of the quasi-particle operators $(d_{\boldsymbol{p}\eta;i}, d^{\dagger}_{\boldsymbol{p}\eta;i})$ such as

$$\begin{aligned}
\sum_\alpha c^{\dagger}_{\boldsymbol{p}\eta\alpha u} c_{\boldsymbol{p}-\eta\alpha u} &= c^{\dagger}_{\boldsymbol{p}\eta 1u} c_{\boldsymbol{p}-\eta 1u} + c^{\dagger}_{\boldsymbol{p}\eta 2u} c_{\boldsymbol{p}-\eta 2u} + c^{\dagger}_{\boldsymbol{p}\eta 3u} c_{\boldsymbol{p}-\eta 3u} \\
&= \left[x_p^{(1)} d^{\dagger}_{\boldsymbol{p}\eta;1} + x_p^{(2)} d^{\dagger}_{\boldsymbol{p}\eta;2} + x_p^{(3)} d^{\dagger}_{\boldsymbol{p}\eta;3} - (y_p^{(1)} d_{-\boldsymbol{p}\eta;1} + y_p^{(2)} d_{-\boldsymbol{p}\eta;2} + y_p^{(3)} d_{-\boldsymbol{p}\eta;3})\right] \\
&\quad \times \left[x_p^{(1)} d_{\boldsymbol{p}-\eta;1} + x_p^{(2)} d_{\boldsymbol{p}-\eta;2} + x_p^{(3)} d_{\boldsymbol{p}-\eta;3} \right. \\
&\qquad \left. - (y_p^{(1)} d^{\dagger}_{-\boldsymbol{p}-\eta;1} + y_p^{(2)} d^{\dagger}_{-\boldsymbol{p}-\eta;2} + y_p^{(3)} d^{\dagger}_{-\boldsymbol{p}-\eta;3})\right] \\
&\quad + \left(X_p d^{\dagger}_{\boldsymbol{p}\eta 2u} - Y_p d_{-\boldsymbol{p}\eta 1d}\right)\left(X_p d_{\boldsymbol{p}-\eta 2u} - Y_p d_{-\boldsymbol{p}-\eta 1d}\right) \\
&\quad + \left(X_p d^{\dagger}_{\boldsymbol{p}\eta 3u} - Y_p d_{-\boldsymbol{p}\eta 1s}\right)\left(X_p d_{\boldsymbol{p}-\eta 3u} - Y_p d_{-\boldsymbol{p}-\eta 1s}\right).
\end{aligned} \tag{5.3}$$

Therefore, the intermediate states $|i\rangle$ are needed:

$$|i\rangle = |\boldsymbol{p}\eta ab\rangle \equiv d^{\dagger}_{\boldsymbol{p}\eta;a} d^{\dagger}_{-\boldsymbol{p}-\eta;b}|\Phi\rangle \quad (\langle i| = \langle\Phi|d_{-\boldsymbol{p}-\eta;b} d_{\boldsymbol{p}\eta;a}). \tag{5.4}$$

Here, we remember that $d_{\boldsymbol{p}\eta;4} = d_{\boldsymbol{p}\eta 2u}$, and so on. We summarize the necessary pieces to calculate the second-order perturbative correction of energy for $\epsilon_p > \mu$ in Appendix B. Thus, for $\epsilon_p > \mu$, the

second-order perturbative correction, $E^{>}_{\rm corr}$, for the energy can be expressed as

$$
\begin{aligned}
E^{>}_{\rm corr} &= \sum_{\boldsymbol{p}\eta ab} \frac{\langle\Phi|H_1|\boldsymbol{p}\eta ab\rangle\langle\boldsymbol{p}\eta ab|H_1|\Phi\rangle}{E_0 - E_{\boldsymbol{p}\eta ab}} \\
&= -\sum_{\boldsymbol{p}\eta(\epsilon>\mu)} \Bigg\{ \frac{(e_u+e_d+e_s)^2 (x_p^{(1)} y_p^{(1)})^2}{2\sqrt{\bar{\epsilon}^2+4\Delta^2}} \\
&\qquad + \frac{1}{\sqrt{\bar{\epsilon}^2+4\Delta^2}+\sqrt{\bar{\epsilon}^2+\Delta^2}} \Big[(e_u-e_d)^2 (x_p^{(2)} y_p^{(1)} \\
&\qquad\qquad + x_p^{(1)} y_p^{(2)})^2 + (e_u+e_d-2e_s)^2 (x_p^{(1)} y_p^{(3)} + x_p^{(3)} y_p^{(1)})^2 \Big] \\
&\qquad + \frac{1}{2\sqrt{\bar{\epsilon}^2+\Delta^2}} \Big[(e_u+e_d)^2 (x_p^{(2)} y_p^{(2)})^2 \\
&\qquad\qquad + (e_u-e_d)^2 (x_p^{(2)} y_p^{(3)} + x_p^{(3)} y_p^{(2)})^2 + (e_u+e_d+4e_s)^2 (x_p^{(3)} y_p^{(3)})^2 \Big] \\
&\qquad + \frac{1}{2\sqrt{\bar{\epsilon}^2+\Delta^2}} \Big[(e_u+e_d)^2 + (e_u+e_s)^2 + (e_d+e_s)^2 \Big] (X_p Y_p)^2 \Bigg\}. \qquad (5.5)
\end{aligned}
$$

As for the case $\epsilon_p < \mu$, the same results are derived. The intermediate states are adopted as

$$
|\boldsymbol{p}\eta\overline{ab}\rangle = \bar{d}^{\dagger}_{-\boldsymbol{p}\eta;a} \bar{d}^{\dagger}_{\boldsymbol{p}-\eta;b} |\Phi\rangle \ . \qquad (5.6)
$$

Then, the structure of operators in H_1 for $\epsilon_p < \mu$ is the same as that of the case for $\epsilon_p > \mu$. Thus, the correction energy, $E^{<}_{\rm corr}$, for $\epsilon_p < \mu$ has the same form:

$$
\begin{aligned}
E^{<}_{\rm corr} &= \sum_{\boldsymbol{p}\eta ab} \frac{\langle\Phi|H_1|\boldsymbol{p}\eta\overline{ab}\rangle\langle\boldsymbol{p}\eta\overline{ab}|H_1|\Phi\rangle}{E_0 - E_{\boldsymbol{p}\eta\overline{ab}}} \\
&= -\sum_{\boldsymbol{p}\eta(\epsilon<\mu)} \Bigg\{ \frac{(e_u+e_d+e_s)^2 (\bar{x}_p^{(1)} \bar{y}_p^{(1)})^2}{2\sqrt{\bar{\epsilon}^2+4\Delta^2}} \\
&\qquad + \frac{1}{\sqrt{\bar{\epsilon}^2+4\Delta^2}+\sqrt{\bar{\epsilon}^2+\Delta^2}} \Big[(e_u-e_d)^2 (\bar{x}_p^{(2)} \bar{y}_p^{(1)} \\
&\qquad\qquad + \bar{x}_p^{(1)} \bar{y}_p^{(2)})^2 + (e_u+e_d-2e_s)^2 (\bar{x}_p^{(1)} \bar{y}_p^{(3)} + \bar{x}_p^{(3)} \bar{y}_p^{(1)})^2 \Big] \\
&\qquad + \frac{1}{2\sqrt{\bar{\epsilon}^2+\Delta^2}} \Big[(e_u+e_d)^2 (\bar{x}_p^{(2)} \bar{y}_p^{(2)})^2 \\
&\qquad\qquad + (e_u-e_d)^2 (\bar{x}_p^{(2)} \bar{y}_p^{(3)} + \bar{x}_p^{(3)} \bar{y}_p^{(2)})^2 + (e_u+e_d+4e_s)^2 (\bar{x}_p^{(3)} \bar{y}_p^{(3)})^2 \Big] \\
&\qquad + \frac{1}{2\sqrt{\bar{\epsilon}^2+\Delta^2}} \Big[(e_u+e_d)^2 + (e_u+e_s)^2 + (e_d+e_s)^2 \Big] (\bar{X}_p \bar{Y}_p)^2 \Bigg\}. \qquad (5.7)
\end{aligned}
$$

Finally, we obtain the correction energy by the second-order perturbation as

$$
E_{\rm corr} = E^{>}_{\rm corr} + E^{<}_{\rm corr}. \qquad (5.8)
$$

Here, by using $x_p^{(a)}$, $y_p^{(a)}$, X_p, Y_p in (3.7), $\bar{x}_p^{(a)}$, $\bar{y}_p^{(a)}$, $\bar{X}_p$, $\bar{Y}_p$ in (3.8), e_τ in (5.1), and $\mathcal{F}_\tau$ in (2.2), and by substituting the above quantities into $E_{\rm corr}$, we obtain

$$E_{\rm corr} = -2\left(\sum_{\boldsymbol{p}\ (\epsilon>\mu)} + \sum_{\boldsymbol{p}\ (\epsilon<\mu)}\right)\frac{p_1^2+p_2^2}{|\boldsymbol{p}|^2}\left\{\frac{1}{\sqrt{\bar{\epsilon}^2+4\Delta^2}+\sqrt{\bar{\epsilon}^2+\Delta^2}}\right.$$
$$\times\frac{1}{3}\left(1-\frac{\bar{\epsilon}^2+2\Delta^2}{\sqrt{\bar{\epsilon}^2+\Delta^2}\sqrt{\bar{\epsilon}^2+4\Delta^2}}\right)\cdot\left(F_3^2+F_8^2\right)$$
$$\left.+\frac{1}{2\sqrt{\bar{\epsilon}^2+\Delta^2}}\cdot\frac{\Delta^2}{\bar{\epsilon}^2+\Delta^2}\left(\frac{5}{6}F_3^2+\frac{19}{12}F_8^2\right)\right\}. \quad (5.9)$$

Then the thermodynamic potential Φ can be obtained up to the second order of $V_{\rm SP}$, namely, up to the second order of F_k, as

$$\Phi = \Phi_0 + \frac{1}{V}\cdot E_{\rm corr} + \frac{1}{2G}(F_3^2+F_8^2). \quad (5.10)$$

The order of the phase transition from CFL to SP phases is determined through (5.9). Namely, from (5.9) and (5.10), for the CFL phase, but with small F_3 and/or F_8, the thermodynamic potential Φ is obtained as

$$\Phi = \Phi_0 + \left(c_3+\frac{1}{2G}\right)F_3^2 + \left(c_8+\frac{1}{2G}\right)F_8^2 \quad (5.11)$$

up to the second order of F_k. Here, c_3 and c_8 are expressed as

$$c_3 = -\frac{1}{\pi^2}\int_0^\Lambda dp_3\int_0^{\sqrt{\Lambda^2-p_3^2}} dp_\perp\, p_\perp$$
$$\times\left[\frac{p_\perp^2}{|\boldsymbol{p}|^2}\left\{\frac{1}{\sqrt{|\boldsymbol{p}|^2-2\mu|\boldsymbol{p}|+\mu^2+4\Delta^2}+\sqrt{|\boldsymbol{p}|^2-2\mu|\boldsymbol{p}|+\mu^2+\Delta^2}}\right.\right.$$
$$\times\frac{1}{3}\left(1-\frac{|\boldsymbol{p}|^2-2\mu|\boldsymbol{p}|+\mu^2+2\Delta^2}{\sqrt{|\boldsymbol{p}|^2-2\mu|\boldsymbol{p}|+\mu^2+4\Delta^2}\sqrt{|\boldsymbol{p}|^2-2\mu|\boldsymbol{p}|+\mu^2+\Delta^2}}\right)$$
$$\left.\left.+\frac{\Delta^2}{2(|\boldsymbol{p}|^2-2\mu|\boldsymbol{p}|+\mu^2+\Delta^2)^{3/2}}\cdot\frac{5}{6}\right\}\right],$$
$$c_8 = -\frac{1}{\pi^2}\int_0^\Lambda dp_3\int_0^{\sqrt{\Lambda^2-p_3^2}} dp_\perp\, p_\perp$$
$$\times\left[\frac{p_\perp^2}{|\boldsymbol{p}|^2}\left\{\frac{1}{\sqrt{|\boldsymbol{p}|^2-2\mu|\boldsymbol{p}|+\mu^2+4\Delta^2}+\sqrt{|\boldsymbol{p}|^2-2\mu|\boldsymbol{p}|+\mu^2+\Delta^2}}\right.\right.$$
$$\times\frac{1}{3}\left(1-\frac{|\boldsymbol{p}|^2-2\mu|\boldsymbol{p}|+\mu^2+2\Delta^2}{\sqrt{|\boldsymbol{p}|^2-2\mu|\boldsymbol{p}|+\mu^2+4\Delta^2}\sqrt{|\boldsymbol{p}|^2-2\mu|\boldsymbol{p}|+\mu^2+\Delta^2}}\right)$$
$$\left.\left.+\frac{\Delta^2}{2(|\boldsymbol{p}|^2-2\mu|\boldsymbol{p}|+\mu^2+\Delta^2)^{3/2}}\cdot\frac{19}{12}\right\}\right]. \quad (5.12)$$

If $c_3+1/(2G)>0$ and $c_8+1/(2G)>0$, the phase transition from CFL to SP phases is of the first order because $F_3=F_8=0$ always gives a local minimum of the thermodynamic potential Φ_0. On the other hand, if $c_3+1/(2G)>0$ and $c_8+1/(2G)<0$ and vice versa, or $c_3+1/(2G)<0$ and $c_8+1/(2G)<0$, the phase transition from CFL to SP phases is maybe of the second order. As is seen in

Table 3. The coefficients of F_3^2 $(c_3 + 1/(2G))$ and F_8^2 $(c_8 + 1/(2G))$ are numerically given within the second-order perturbation theory at each chemical potential μ.

μ/GeV	$c_3 + 1/(2G)$	$c_8 + 1/(2G)$
0.40	0.015734	0.0076297
0.41	0.015304	0.0068182
0.42	0.014873	0.0060047
0.43	0.014427	0.0051920
0.44	0.014015	0.0043828
0.45	0.013592	0.0035803
0.4558	0.0133487	0.0031934
0.46	0.013174	0.0027882
0.47	0.012765	0.0020104
0.48	0.012367	0.0012519
0.49	0.011982	0.00051816
0.50	0.116142	−0.00018406

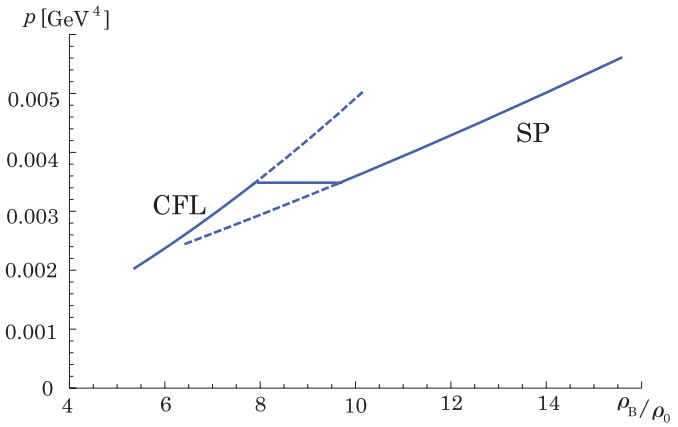

Fig. 4. The pressure is depicted as a function of the baryon number density divided by the normal nuclear density. The solid curve represents the realized phase.

Table 3, in the region of $\mu \leq 0.49$ GeV, and in particular at $\mu = \mu_c$ $(= 0.4558$ GeV), the coefficients $c_3 + 1/(2G)$ and $c_8 + 1/(2G)$ are positive. Thus, the phase transition may be of the first order.

From the above consideration, in Fig. 4 the pressure is depicted as a function of the baryon number density divided by normal nuclear density, which has already given in Table 2. The realized phase is represented by the solid curve.

6. Summary and concluding remarks

In this paper, it has been shown that quark spin polarization for each flavor may occur in the three-flavor case at high baryon density, which leads to the quark spin-polarized phase, against the color–flavor-locked phase due to the four-point tensor-type interaction between quarks in the Nambu–Jona-Lasinio model. In a certain region of quark chemical potential, the CFL phase is favorable energetically. However, as the quark chemical potential increases, the phase transition from CFL phase to spin-polarized phase occurs. In our theoretical model, the phase transition occurs around the quark chemical potential, being around 0.45 GeV under a certain parameter set. Based on the CFL phase, we have treated the tensor-type interaction term between quarks as a perturbation one. As a result, it has been shown that the phase transition may be of the first order up to the second-order perturbation.

It has also been shown that, owing to the four-point tensor-type interaction, the spin polarization may occur in the NJL model. The tensor-type interaction may come from the two-gluon exchange term between quarks in QCD. It is interesting to clarify the origin of the tensor-type interaction. In this paper, the total spin polarization is not realized, while the spin polarization with respect to each flavor actually occurs. It may be important to introduce quark-mass splitting, namely, the strange quark mass should be taken into account, while we have ignored it in this paper. Further, if the chiral symmetry is explicitly broken, namely, the quark masses are not zero even in the chiral symmetric phase, spin polarization originating from the pseudovector-type four-point interaction between quarks may exist. One of next interesting problems may be to investigate the interplay between the spin polarization from tensor-type interaction and that from the pseudovector-type interaction. As for a realistic calculation of the inner core of neutron stars or quark stars, the charge neutrality condition is important [16], and then the chemical potential of each quark flavor should be introduced. This is one of the future problems we will consider, while we expect that the spin-polarized phase may appear by the effects developed in this paper. Further, it is interesting to investigate the origin of the strong magnetic field [17,18], for example, in the core of neutron stars. It is suggested that, in general, spin polarization leads to the ferromagnetization. It is expected that the strong magnetic field exists in the core of neutron stars. Then, if high-density quark matter is realized in the inner core of neutron stars or quark stars, spin polarization may occur as is shown in this paper. Thus, one direction of investigations in high-density quark matter is to understand whether the quark ferromagnetization is realized or not in the quark spin-polarized phase. This will be one thing to solve.

Acknowledgements

Y.T. would like to express his sincere thanks to Professor J. da Providência and Professor C. Providência, two of the co-authors of this paper, for their warm hospitality during his visit to Coimbra in spring of 2014. Y.T. is partially supported by Grants-in-Aid for Scientific Research (No.23540311, No.26400277) from the Ministry of Education, Culture, Sports, Science, and Technology in Japan.

Funding

Open Access funding: SCOAP[3].

Appendix A. Mean field Hamiltonian without spin polarization in terms of the quasi-particle operators

The mean field Hamiltonian, $H_{\rm eff}$, in (3.1) can be expressed in terms of the quasi-particle operators $d_{p;i}$, $d^\dagger_{p;i}$, $\bar{d}_{\bar{p};i}$, and $\bar{d}^\dagger_{\bar{p};i}$. The result is as follows:

$$
\begin{aligned}
H_{\rm eff} &= H_> + H_< + V\cdot\frac{3\Delta^2}{2G_c},\\
H_> &= \frac{1}{2}\sum_{p\ (\epsilon_p>\mu)}(4\bar{\epsilon}_p^2 Y_p^2 + 4\Delta X_p Y_p \phi_p)\times 3\\
&\quad + \frac{1}{2}\sum_{p\ (\epsilon_p>\mu)}\left[\bar{\epsilon}_p\cdot 6(y_p^{(1)2}+y_p^{(2)2}+y_p^{(3)2}) + 2\Delta(-6x_p^{(1)}y_p^{(1)}+2x_p^{(2)}y_p^{(2)}+6x_p^{(3)}y_p^{(3)})\phi_p\right]\\
&\quad + \sum_{p\ (\epsilon_p>\mu)}\left\{\left[\bar{\epsilon}_p\cdot 3(x_p^{(1)2}-y_p^{(1)2}) + 12\Delta x_p^{(1)}y_p^{(1)}\phi_p\right]d^\dagger_{p;1}d_{p;1}\right.\\
&\qquad \left. + \left[\bar{\epsilon}_p\cdot 2(x_p^{(2)2}-y_p^{(2)2}) - 4\Delta x_p^{(2)}y_p^{(2)}\phi_p\right]d^\dagger_{p;2}d_{p;2}\right.
\end{aligned}
$$

$$
\begin{aligned}
&+\left[\bar{\epsilon}_p\cdot 6(x_p^{(3)2}-y_p^{(3)2})-12\Delta x_p^{(3)}y_p^{(3)}\phi_p\right]d^\dagger_{p;3}d_{p;3}\\
&\quad+\sum_{a=4}^{9}\left[\bar{\epsilon}_p\cdot(X_p^2-Y_p^2)-2\Delta X_pY_p\phi_p\right]d^\dagger_{p;a}d_{p;a}\Bigg\}\\
&+\sum_{p\ (\epsilon_p>\mu)}\Bigg\{\left[-6\bar{\epsilon}_p x_p^{(1)}y_p^{(1)}+6\Delta(x_p^{(1)2}-y_p^{(1)2})\phi_p\right](d^\dagger_{p;1}d^\dagger_{\bar{p};1}+d_{\bar{p};1}d_{p1})\\
&\quad+\left[-4\bar{\epsilon}_p x_p^{(2)}y_p^{(2)}-2\Delta(x_p^{(2)2}-y_p^{(2)2})\phi_p\right](d^\dagger_{p;2}d^\dagger_{\bar{p};2}+d_{\bar{p};2}d_{p2})\\
&\quad+\left[-12\bar{\epsilon}_p x_p^{(3)}y_p^{(3)}-6\Delta(x_p^{(3)2}-y_p^{(3)2})\phi_p\right](d^\dagger_{p;3}d^\dagger_{\bar{p};3}+d_{\bar{p};3}d_{p3})\\
&\quad+\left[-2\bar{\epsilon}_p X_pY_p-\Delta(X_p^2-Y_p^2)\phi_p\right]\\
&\qquad\times(d^\dagger_{p2u}d^\dagger_{\bar{p}1d}+d^\dagger_{p1d}d^\dagger_{\bar{p}2u}+d_{\bar{p}1d}d_{p2u}+d_{\bar{p}2u}d_{p1d}+d^\dagger_{p3u}d^\dagger_{\bar{p}1s}+d^\dagger_{p1s}d^\dagger_{\bar{p}3u}\\
&\qquad\quad+d_{\bar{p}1s}d_{p3u}+d_{\bar{p}3u}d_{p1s}+d^\dagger_{p3d}d^\dagger_{\bar{p}2s}+d^\dagger_{p2s}d^\dagger_{\bar{p}3d}+d_{\bar{p}2s}d_{p3d}+d_{\bar{p}3d}d_{p2s})\Bigg\},
\end{aligned}
$$

$$
\begin{aligned}
H_<=&\frac{1}{2}\sum_{p\ (\epsilon_p<\mu)}(4\bar{\epsilon}_p^2\bar{X}_p^2-4\Delta\bar{X}_p\bar{Y}_p\phi_p)\times 3\\
&+\frac{1}{2}\sum_{p\ (\epsilon_p<\mu)}\left[\bar{\epsilon}_p\cdot 2(3\bar{x}_p^{(1)2}+2\bar{x}_p^{(2)2}+6\bar{x}_p^{(3)2})+2\Delta(6\bar{x}_p^{(1)}y_p^{(1)}-2\bar{x}_p^{(2)}\bar{y}_p^{(2)}-6\bar{x}_p^{(3)}\bar{y}_p^{(3)})\phi_p\right]\\
&+\sum_{p\ (\epsilon_p<\mu)}\Bigg\{\left[\bar{\epsilon}_p\cdot 3(\bar{y}_p^{(1)2}-\bar{x}_p^{(1)2})-12\Delta\bar{x}_p^{(1)}\bar{y}_p^{(1)}\phi_p\right]\bar{d}^\dagger_{p;1}\bar{d}_{p;1}\\
&\quad+\left[\bar{\epsilon}_p\cdot 2(\bar{y}_p^{(2)2}-\bar{x}_p^{(2)2})+4\Delta\bar{x}_p^{(2)}\bar{y}_p^{(2)}\phi_p\right]\bar{d}^\dagger_{p;2}\bar{d}_{p;2}\\
&\quad+\left[\bar{\epsilon}_p\cdot 6(\bar{y}_p^{(3)2}-\bar{x}_p^{(3)2})+12\Delta\bar{x}_p^{(3)}\bar{y}_p^{(3)}\phi_p\right]\bar{d}^\dagger_{p;3}\bar{d}_{p;3}\\
&\quad+\sum_{a=4}^{9}\left[\bar{\epsilon}_p\cdot(\bar{Y}_p^2-\bar{X}_p^2)+2\Delta\bar{X}_p\bar{Y}_p\phi_p\right]\bar{d}^\dagger_{p;a}\bar{d}_{p;a}\Bigg\}\\
&+\sum_{p\ (\epsilon_p<\mu)}\Bigg\{\left[-6\bar{\epsilon}_p\bar{x}_p^{(1)}\bar{y}_p^{(1)}+6\Delta(\bar{x}_p^{(1)2}-\bar{y}_p^{(1)2})\phi_p\right](\bar{d}_{\bar{p};1}\bar{d}_{p;1}+\bar{d}^\dagger_{p;1}\bar{d}^\dagger_{\bar{p};1})\\
&\quad+\left[-4\bar{\epsilon}_p\bar{x}_p^{(2)}\bar{y}_p^{(2)}-2\Delta(\bar{x}_p^{(2)2}-\bar{y}_p^{(2)2})\phi_p\right](\bar{d}_{\bar{p};2}\bar{d}_{p;2}+\bar{d}^\dagger_{p;2}\bar{d}^\dagger_{\bar{p};2})\\
&\quad+\left[-12\bar{\epsilon}_p\bar{x}_p^{(3)}\bar{y}_p^{(3)}-6\Delta(\bar{x}_p^{(3)2}-\bar{y}_p^{(3)2})\phi_p\right](\bar{d}_{\bar{p};3}\bar{d}_{p;3}+\bar{d}^\dagger_{p;3}\bar{d}^\dagger_{\bar{p};3})\\
&\quad+\left[-2\bar{\epsilon}_p\bar{X}_p\bar{Y}_p-\Delta(\bar{X}_p^2-\bar{Y}_p^2)\phi_p\right]\\
&\qquad\times(\bar{d}_{\bar{p}2u}\bar{d}_{p1d}+\bar{d}_{\bar{p}1d}\bar{d}_{p2u}+\bar{d}^\dagger_{p1d}\bar{d}^\dagger_{\bar{p}2u}+\bar{d}^\dagger_{p2u}\bar{d}^\dagger_{\bar{p}1d}+\bar{d}_{\bar{p}3u}\bar{d}_{p1s}+\bar{d}_{\bar{p}1s}\bar{d}_{p3u}\\
&\qquad\quad+\bar{d}^\dagger_{p1s}\bar{d}^\dagger_{\bar{p}3u}+\bar{d}^\dagger_{p3u}\bar{d}^\dagger_{\bar{p}1s}+\bar{d}_{\bar{p}3d}\bar{d}_{p2s}+\bar{d}_{\bar{p}2s}\bar{d}_{p3d}+\bar{d}^\dagger_{p2s}\bar{d}^\dagger_{\bar{p}3d}+\bar{d}^\dagger_{p3d}\bar{d}^\dagger_{\bar{p}2s})\Bigg\}.
\end{aligned}
\tag{A1}
$$

Substituting $x_p^{(a)}$ and so on, we obtain the simple form in (3.12).

Appendix B. Necessary matrix elements in the second-order perturbation theory

We collect the necessary pieces to calculate the second-order correction of energy, (5.2).

$$
\begin{aligned}
\langle\Phi|H_1|\boldsymbol{p}\eta 11\rangle\langle\boldsymbol{p}\eta 11|H_1|\Phi\rangle &= \sum_{\boldsymbol{p}'\eta'}\langle\Phi|(-x^{(1)}_{p'}y^{(1)}_{p'})(e_u+e_d+e_s)d_{-\boldsymbol{p}'\eta';1}d_{\boldsymbol{p}'-\eta';1}\cdot d^{\dagger}_{\boldsymbol{p}\eta;1}d^{\dagger}_{-\boldsymbol{p}-\eta;1}|\Phi\rangle \\
&\quad\times\sum_{\boldsymbol{p}'\eta'}\langle\Phi|d_{-\boldsymbol{p}-\eta;1}d_{\boldsymbol{p}\eta;1}(-x^{(1)}_{p'}y^{(1)}_{p'})(e_u+e_d+e_s)d^{\dagger}_{\boldsymbol{p}'\eta';1}d^{\dagger}_{-\boldsymbol{p}'-\eta';1}|\Phi\rangle \\
&= (x^{(1)}_p y^{(1)}_p)^2(e_u+e_d+e_s)^2, \\
E_0-E_{11} &= -2\sqrt{\bar{\epsilon}^2+4\Delta^2}, \\
\langle\Phi|H_1|\boldsymbol{p}\eta 12\rangle\langle\boldsymbol{p}\eta 12|H_1|\Phi\rangle &= (x^{(2)}_p y^{(1)}_p + x^{(1)}_p y^{(2)}_p)^2(-e_u+e_d)^2, \\
E_0-E_{12} &= -\sqrt{\bar{\epsilon}^2+4\Delta^2}-\sqrt{\bar{\epsilon}^2+\Delta^2}, \\
\langle\Phi|H_1|\boldsymbol{p}\eta 13\rangle\langle\boldsymbol{p}\eta 13|H_1|\Phi\rangle &= (x^{(1)}_p y^{(3)}_p + x^{(3)}_p y^{(1)}_p)^2(-e_u-e_d+2e_s)^2, \\
E_0-E_{13} &= -\sqrt{\bar{\epsilon}^2+4\Delta^2}-\sqrt{\bar{\epsilon}^2+\Delta^2}, \\
\langle\Phi|H_1|\boldsymbol{p}\eta 22\rangle\langle\boldsymbol{p}\eta 22|H_1|\Phi\rangle &= (x^{(2)}_p y^{(2)}_p)^2(e_u+e_d)^2, \\
E_0-E_{22} &= -2\sqrt{\bar{\epsilon}^2+\Delta^2}, \\
\langle\Phi|H_1|\boldsymbol{p}\eta 23\rangle\langle\boldsymbol{p}\eta 23|H_1|\Phi\rangle &= (x^{(2)}_p y^{(3)}_p + x^{(3)}_p y^{(2)}_p)^2(-e_u+e_d)^2, \\
E_0-E_{23} &= -2\sqrt{\bar{\epsilon}^2+4\Delta^2}, \\
\langle\Phi|H_1|\boldsymbol{p}\eta 33\rangle\langle\boldsymbol{p}\eta 33|H_1|\Phi\rangle &= (x^{(3)}_p y^{(3)}_p)^2(e_u+e_d+4e_s)^2, \\
E_0-E_{33} &= -2\sqrt{\bar{\epsilon}^2+4\Delta^2}, \\
\langle\Phi|H_1|\boldsymbol{p}\eta 45\rangle\langle\boldsymbol{p}\eta 45|H_1|\Phi\rangle &= (X_p Y_p)^2(e_u+e_d)^2, \\
E_0-E_{45} &= -2\sqrt{\bar{\epsilon}^2+4\Delta^2}, \\
\langle\Phi|H_1|\boldsymbol{p}\eta 67\rangle\langle\boldsymbol{p}\eta 67|H_1|\Phi\rangle &= (X_p Y_p)^2(e_u+e_s)^2, \\
E_0-E_{67} &= -2\sqrt{\bar{\epsilon}^2+4\Delta^2}, \\
\langle\Phi|H_1|\boldsymbol{p}\eta 89\rangle\langle\boldsymbol{p}\eta 89|H_1|\Phi\rangle &= (X_p Y_p)^2(e_d+e_s)^2, \\
E_0-E_{89} &= -2\sqrt{\bar{\epsilon}^2+4\Delta^2}.
\end{aligned}
\tag{B1}
$$

References

[1] K. Fukushima and T. Hatsuda, Rep. Prog. Phys. **74**, 014001 (2011).
[2] M. G. Alford, A. Schmitt, K. Rajagopal, and T. Schafer, Rev. Mod. Phys. **80**, 1455 (2008), and references cited therein.
[3] T. Tatsumi, Phys. Lett. B **489**, 280 (2000).
[4] T. Maruyama and T. Tatsumi, Nucl. Phys. A **693**, 710 (2001).
[5] E. Nakano, T. Maruyama, and T. Tatsumi, Phys. Rev. D **68**, 105001 (2003).
[6] S. Maedan, Prog. Theor. Phys. **118**, 729 (2007).
[7] Y. Tsue, J. da Providência, C. Providência, and M. Yamamura, Prog. Theor. Phys. **128**, 507 (2012).
[8] Y. Nambu and G. Jona-Lasinio, Phys. Rev. **122**, 345 (1961).
[9] Y. Nambu and G. Jona-Lasinio, Phys. Rev. **124**, 246 (1961).
[10] H. Bohr, P. K. Panda, C. Providência, and J. da Providência, Int. J. Mod. Phys. E **22**, 1350019 (2013).
[11] Y. Tsue, J. da Providência, C. Providência, M. Yamamura, and H. Bohr, Prog. Theor. Exp. Phys. **10**, 103D01 (2013).

[12] M. Kobayashi and T. Maskawa, Prog. Theor. Phys. **44**, 1422 (1970).
[13] G. 't Hooft, Phys. Rev. D **14**, 3432 (1976).
[14] H. Bohr, C. Providência, and J. da Providência, Eur. Phys. J. A **41**, 355 (2009).
[15] H. Bohr, P. K. Panda, C. Providência, and J. da Providência, Braz. J. Phys. **42**, 68 (2012).
[16] M. Alford and K. Rajagopal, JHEP **0206**, 031 (2002).
[17] A. Iwazaki, Phys. Rev. D **72**, 114003 (2005).
[18] E. J. Ferrer, V. de la Incera, I. Portillo, and M. Quiroz, [arXiv:1311.3400v3] .